*Final version available here: http://dx.doi.org/10.1130/B31136.1*



# Paleozoic evolution of western Marie Byrd Land, Antarctica

**Chris Yakymchuk**[†]
**Caitlin R. Brown**
**Michael Brown**
*Laboratory For Crustal Petrology, Department of Geology, University of Maryland, College Park, Maryland 20742, USA*

**Christine S. Siddoway**
*Department of Geology, The Colorado College, Colorado Springs, Colorado 80903, USA*

**C. Mark Fanning**
*Research School of Earth Sciences, The Australian National University, Mills Road, Canberra ACT 0200, Australia*

**Fawna J. Korhonen**
*Geological Survey of Western Australia, East Perth WA 6004, Australia*

[†]Current address: Department of Earth and Environmental Sciences, University of Waterloo, 200 University Avenue West, Waterloo, Ontario, N2L 3G1, Canada.
email: cyakymchuk@uwaterloo.ca

**Keywords:** Antarctica, Hf and O isotopes, zircon, granite, Gondwana

## ABSTRACT

We report geochemical data from (meta-)sedimentary and igneous rocks that crop out in the Ford Ranges of western Marie Byrd Land and discuss the evolution and reworking of the crust in this region during Paleozoic subduction along the former Gondwanan convergent plate margin. Detrital zircon age spectra from the Swanson Formation, a widespread low-grade metaturbidite sequence, define distinct populations in the late Paleoproterozoic, late Mesoproterozoic and Neoproterozoic–Cambrian. The late Paleoproterozoic group records magmatism derived from a mixed juvenile and crustal source. By contrast, the late Mesoproterozoic group yields Hf isotope values consistent with derivation from a juvenile Mesoproterozoic source inferred to be an unexposed Grenville-age orogenic belt beneath the East Antarctic ice sheet. For the Neoproterozoic–Cambrian population, Hf isotope values indicate reworking of these older materials during Ross–Delamerian orogenesis. New U–Pb ages from the Devonian–Carboniferous Ford Granodiorite suite across the Ford Ranges reveal an extended period of arc magmatism from 375 to 345 Ma. For four younger samples of Ford Granodiorite, Hf and O isotope values in zircon suggest involvement of a larger (meta-)sedimentary component in the petrogenesis than for two older samples. This contrasts with the secular trend towards more juvenile values documented from Silurian to Permian granite suites in the Tasmanides of eastern Australia and Famennian to Tournasian granite suites in New Zealand, pieces of continental crust that were once contiguous with western Marie Byrd Land along the Gondwana margin. The differences may relate to an along-arc change from the typical extensional accretionary mode in eastern Australia to a neutral or an advancing mode in West Antarctica, and to an across-arc difference in distance from the trench between the New Zealand fragments of Zealandia and western Marie Byrd Land. Upper Devonian anatectic granites in the Ford Ranges most likely record reworking of early Ford Granodiorite suite members during arc magmatism.

## INTRODUCTION

The former continental margin of Gondwana represents one of the most long-lived and extensive active convergent plate margins in the Phanerozoic (e.g. Cawood, 2005; Collins et al., 2011; Harley et al., 2013). Information about the evolution and reworking of the East Gondwanan segment is recorded in the geology and geochemistry of the sedimentary, igneous and metamorphic rocks that crop out in different regions that were once contiguous (Fig. 1A), including: the Tasmanides of Eastern Australia; the Western Province of New Zealand; north Victoria Land; Marie Byrd Land; the Antarctic Peninsula; and the western margin of South America. The New Zealand–Antarctica segment of the former active margin links the geology of eastern Australia to the east (present co-ordinates) to that of the Antarctic Peninsula and South America to the west (present co-ordinates). The relatively well-understood Tasmanides in eastern Australia represent the type example of an extensional accretionary orogen (Collins, 2002). However, it is of interest to know how the tectonic evolution of this margin might have changed along strike to the west. In Antarctica, the relatively simple Paleozoic tectonic history of western Marie Byrd Land, compared to north Victoria Land (e.g. Borg et al., 1986), makes Marie Byrd Land an ideal location for characterization of the Paleozoic history of the Marie Byrd Land–Zealandia portion of the East Gondwana accretionary margin. Well-substantiated ties between Marie Byrd Land–Zealandia and Zealandia–Australia span the Paleozoic and Mesozoic (Bradshaw et. 1997; Ireland et al. 1998; Wandres and Bradshaw, 2005; Adams, 2010); hence this study contributes significant new data with bearing on the integrated margin. Thus, the results of the study we report herein enable a comparison with the well-characterized evolutionary history of eastern Australia and with recently published data from the formerly contiguous parts of New Zealand.

The scarcity of outcrop and difficulty of access in West Antarctica due to the extensive ice cover has limited our understanding of the geology of Marie Byrd Land. Based on a few pioneering studies (Pankhurst et al., 1998; Mukasa and Dalziel, 2000), the tectonic history of this region has been inferred from the geochemistry and geochronology of (meta-)sedimentary and igneous rocks exposed as isolated peaks. Outstanding issues to be addressed in western Marie Byrd Land include: 1) the provenance of Cambrian–Ordovician (meta-)sedimentary rocks; 2) the duration of Devonian–Carboniferous magmatism, which is mostly constrained at present by whole-rock Rb–Sr isochron ages; and, 3) the petrogenesis of the Devonian–Carboniferous Ford

Granodiorite suite and associated diatexite (anatectic granite that includes transported residue) and granite.

In this study we report geochemical data from detrital zircons from the Cambrian–Ordovician Swanson Formation and related paragneisses, and for whole rocks and zircons from the Devonian–Carboniferous Ford Granodiorite suite and associated diatexite and granite to investigate crustal evolution and reworking in western Marie Byrd Land. First, we use the U–Pb and Hf isotope values of detrital zircon to evaluate the provenance of Cambrian–Ordovician metasedimentary rocks in the Ford Ranges. Second, we couple zircon and whole-rock geochemical information to constrain the duration and petrogenesis of the Ford Granodiorite suite magmatism and associated diatexite and granite. This new study validates the petrogenetic model proposed by Yakymchuk et al. (2013a) in which the Upper Devonian diatexite and granite are the product of partial melting of both the Swanson Formation and the Ford Granodiorite suite. Finally, we combine this new information with data from the literature from contemporaneous magmatic suites along the former continental margin of Gondwana to address the similarities and differences in the proportion of crustal growth to crustal reworking along a Phanerozoic convergent plate margin system.

## REGIONAL GEOLOGY

Marie Byrd Land in West Antarctica (Fig. 1B) was once contiguous with the Western Province of New Zealand, north Victoria Land, and the Tasmanides of eastern Australia prior to the breakup of the active continental plate margin of Gondwana during the Upper Cretaceous (Fig. 1A). Based on Nd model ages of granites, Pankhurst et al. (1998) divided Marie Byrd Land into the Ross Province in the west and the Amundsen Province in the east. The boundary between the two provinces is unexposed and is believed to be oblique to the present coastline

(Fig. 2; DiVenere et al., 1995; Pankhurst et al., 1998). Paleomagnetic data suggest that these two provinces were amalgamated in the Cretaceous (DiVenere et al., 1995; Luyendyk et al., 1996) prior to the separation of Zealandia from West Antarctica (Fig. 1A).

In the Ford Ranges of the Ross Province (Fig. 1A, B), the Neoproterozoic–Cambrian Swanson Formation is the oldest exposed unit (Bradshaw et al., 1983; Pankhurst et al., 1998; Adams, 1986, 2004). It is a folded and cleaved metaturbidite sequence that accumulated outboard of the Cambrian Ross–Delamerian orogen. In a regional context, based on the similarity of U–Pb ages of detrital zircons, the Swanson Formation has been correlated with the Robertson Bay Group in north Victoria Land and the Greenland Group in the Western Province of New Zealand (Ireland et al., 1998; Adams et al., 2013). Paleocurrent data from the Swanson Formation has been interpreted to suggest flow predominantly towards the North (Bradshaw et al., 1983), indicating a source terrain to the south.

The Swanson Formation is intruded by the Devonian–Carboniferous Ford Granodiorite suite, which was associated with a major pulse of Paleozoic calc-alkaline magmatism along the length of the Antarctica–Zealandia–Australia segment of the Gondwanan continental margin (Weaver et al., 1991; Weaver et al., 1992; Muir et al., 1994; Storey et al., 1999; Mukasa and Dalziel, 2000) that has been variously attributed to subduction (Weaver et al., 1991) or back-arc extension (Muir et al., 1996; Tulloch et al., 2009). Rb–Sr whole-rock geochronology from the Ford Granodiorite suite yielded ages of 380–353 Ma (Adams, 1987). U–Pb ages of ca. 375 and 373 Ma from two Ford Granodiorite suite samples have been used to argue that this magmatism represented only a short-lived pulse of activity (Pankhurst et al., 1998; Yakymchuk et al., 2013a). A broader span for magmatic activity is suggested by U–Pb SHRIMP zircon ages of 369–353 Ma for granites within the Fosdick migmatite–granite complex (Fig. 2, inset; Siddoway and Fanning, 2009) and U–Pb monazite ages of ca. 359 and 351 Ma for two-mica granites (Tulloch et al., 2009). A syenogranite sample from Bruner Hill on the Ruppert coast sampled close to the inferred boundary between the Ross and Amundsen Provinces yielded a U–Pb age of 339 ± 6 Ma (Pankhurst et al., 1998). However, it has remained unclear if these data sampled short-lived magmatic pulses or a protracted magmatic history during the Devonian–Carboniferous. Contemporaneous magmatism is recorded in the Admiralty Intrusives of north Victoria Land (390–350 Ma; Borg et al., 1986; Fioretti et al., 1997), the Karamea suite in the Western Province of New Zealand (371–305 Ma; Tulloch et al., 2009), and in the Melbourne terrane in the Tasmanides of Eastern Australia (ca. 360 Ma; Chappell et al., 1988).

In the Amundsen Province of eastern Marie Byrd Land, Cambrian metasedimentary rocks appear to be absent and magmatism occurred in the Ordovician–Silurian (450–420 Ma) and in the Permian (ca. 276 Ma; Pankhurst et al., 1998). Granites in the Amundsen Province yield younger Nd model ages (1.3–1.0 Ga) than granites from the Ross Province (1.5–1.3 Ga; Pankhurst et al., 1998), which, together with the paleomagnetic evidence (DiVenere et al., 1995; Luyendyk et al., 1996), provided the basis for the subdivision of Marie Byrd Land.

Within the Ford Ranges of western Marie Byrd Land (Fig. 1B), the Fosdick Mountains expose a migmatite–granite complex (Fig. 2, hereafter the Fosdick complex). Paragneisses and orthogneisses within the Fosdick complex are interpreted as the high-grade metamorphosed equivalents of the Swanson Formation and the Ford Granodiorite suite, respectively (Richard et al., 1994; Siddoway and Fanning, 2009; Korhonen et al., 2010a, b; Yakymchuk et al., 2013a, b, 2015). Based on phase equilibria modeling, U–Pb ages of monazite and Lu–Hf ages of garnet, two metamorphic events have been documented in the Fosdick complex, one in the Devonian–Carboniferous and a higher-grade overprint in the Cretaceous (Korhonen et al., 2010b, 2012;

Yakymchuk et al., 2015). Hf and O isotope compositions of zircons from Devonian–Carboniferous granites in the Fosdick complex indicate that they represent a binary mixture sourced from Ford Granodiorite suite and Swanson Formation components (Yakymchuk et al., 2013a). In contrast, Hf and O isotope compositions of zircons from Cretaceous granites indicate input from an unexposed juvenile source in addition to the crustal sources. In general, both the Devonian–Carboniferous and Cretaceous granites in the Ross Province have more evolved Hf isotope values than granites from correlative localities across the Gondwanan margin, including the Western Province of New Zealand and the Tasmanides in eastern Australia. Yakymchuk et al. (2013a) interpreted this difference to record a larger proportion of crustal reworking in the Ross Province compared with a higher proportion of crustal growth in the Western Province and the Tasmanides.

## ANALYTICAL METHODS

A detailed description of analytical methods together with Tables DR1–DR9 listing sample locations and the complete analytical data set are available from the GSA Data Repository. Zircon mineral separates were obtained from bulk rock samples using standard crushing, magnetic, and heavy liquid separation methods in the mineral separation facility at the University of Maryland; zircons were mounted in epoxy disks. The zircons were imaged in transmitted light and studied using a cathodoluminescence detector to characterize the internal zoning of each zircon and to avoid analysis of inclusions

Four Ford Granodiorite suite samples from outside the Fosdick complex in western Marie Byrd Land and two diatexites from inside the Fosdick complex (Table 1, Fig. 2) were selected for zircon U–Pb, O, and Lu–Hf isotope analysis at the Research School of Earth Sciences

(RSES), Australian National University following the protocol given in Yakymchuk et al. (2013a). U–Pb isotope ratios were measured with a SHRIMP–II, oxygen isotope ratios were measured with a SHRIMP–II or SHRIMP-SI, and Lu–Hf measurements were conducted by laser ablation multi-collector inductively coupled plasma mass spectroscopy (LA–MC–ICPMS) using the RSES Neptune MC–ICP–MS coupled with a HelEx 193 nm ArF Excimer laser.

Detrital zircons from two Swanson Formation samples and igneous zircons from two Ford Granodiorite suite samples from outside the Fosdick complex in western Marie Byrd Land, as well as zircons from three paragneisses from outside the Fosdick complex, and two diatexites and one granite from inside the complex (Table 1, Fig. 2) were analyzed for U–Pb LA–MC–ICPMS geochronology at the University of Arizona Laserchron facility following the protocol outlined in Gehrels et al. (2008). Common Pb correction was accomplished by using Hg-corrected $^{204}$Pb and assuming an initial Pb composition from Stacey and Kramers (1975). For the two Swanson Formation samples, Lu and Hf isotopes were also measured in zircon at the University of Arizona Laserchron facility following the procedure described in Cecil et al. (2011). The analyses involve ablation of zircon with a New Wave DUV193 Excimer laser while isotope ratios were measured with a Nu MC–ICPMS.

Strontium, Rb, Nd and Sm isotope compositions for five whole-rock samples of the Swanson Formation, six whole-rock samples of the Ford Granodiorite suite, and three Devonian–Carboniferous granites (Table 1, Fig. 2) were acquired at the University of Maryland using isotope dilution TIMS or ICP–MS following the procedure outlined in Korhonen et al. (2010a). Eight Swanson Formation samples were selected for whole-rock oxygen-isotope analysis at the University of Wisconsin using laser fluorination (Valley et al., 1995).

## SAMPLE DESCRIPTIONS AND U–Pb RESULTS

### Detrital zircons from the Swanson Formation samples and the paragneisses

Representative cathodoluminescence (CL) images of zircons from two Swanson Formation samples are shown in Figure 4. U–Pb results for detrital zircon from the Swanson Formation samples and the paragneisses from the Ford Ranges and Scott Nunataks, including data for one sample reported previously in Yakymchuk et al. (2013a), together with a sample from the Swanson Mountains (Fig. 2) from Adams et al. (2013), are plotted as histograms and normalized probability distributions in Figure 3A–F. In addition, the ages of inherited grains (interpreted as >400 Ma) in the Ford Granodiorite suite, the Devonian–Carboniferous granites and the diatexites are plotted in Figure 3G.

Sample Y2-MD092, from Mount Dolber in the Sarnoff Mountains (Fig. ), is a thinly bedded metagreywacke with a foliation defined by the parallel alignment of biotite. Zircon U–Pb dates range from ca. 440 to ca. 3030 Ma with distribution peaks at 554, 1048 and 1763 Ma (Fig. 3B). The youngest group of four dates that overlap at $\sigma$ yields a weighted mean age of 489 ± 14 Ma.

Sample Y2-MP098, from Mount Passel in the central Ford Ranges (Fig. ), is a poorly sorted metagreywacke containing angular clasts of quartz, feldspar and volcanic rock fragments in a fine-grained matrix. Zircon U–Pb dates range from ca. 510 to ca. 2800 Ma with distribution peaks at 577, 1037 and 1725 Ma (Fig. 3C). The youngest group of four dates that overlap at $\sigma$ yields a weighted mean age of 514.0 ± 4.8 Ma.

Sample 8D27-10 is a calc-silicate gneiss from Mt Woodward in the Ford Ranges (Yakymchuk et al., 2013a). Zircon U–Pb dates range from ca. 500 to ca. 3490 Ma with peaks at 570, 1096, and 1736 Ma (Fig. 3D). The youngest group of four dates that overlap at $\sigma$ yields a weighted mean age of 532.5 ± 5.3 Ma.

Sample 318-M9 is a folded biotite-paragneiss from Mitchell Peak on the Guest Peninsula (Fig. 2). Zircon U–Pb dates range from ca. 330 to ca. 2460 Ma with distribution peaks at 548, 1084 and 1704 Ma (Fig. 3E). The youngest group of four dates that overlap at σ yields a weighted mean age of 509 ± 17 Ma.

Samples 21220-3 and 21220-8 are paragneisses from Scott Nunataks (Smith, 1996). Both samples were collected from the same outcrop, so the age data sets are pooled. Dates range from ca. 110 to ca. 2660 Ma with distribution peaks at 533, 1085, and 1611 Ma as well as a small peak at ca. 412 Ma (Fig. 3F). The youngest group of four dates that overlap at σ yields a weighted mean age of 387 ± 22 Ma.

In summary, individual U–Pb dates for detrital zircons from the Swanson Formation range from ca. 440 to ca. 3030 Ma (Fig. 3A–C); zircons from the paragneisses have similar age distributions, but with a few younger dates (Fig. 3D–F). Although Archean grains are present, they make up only a minor portion of the population. The dominant zircon population in Swanson Formation and paragneiss samples is Neoproterozoic–Cambrian, with dates ranging from ca. 500 to ca. 750 Ma and age peaks at 533 and 576 Ma (Fig. 3A–F). The second significant population comprises mostly Mesoproterozoic dates that range from ca. 930 to ca. 1180 Ma with age peaks at 997 and 1096 Ma (Fig. 3A–F). The third and most poorly defined population comprises mostly Paleoproterozoic dates that extend from ca. 1560 to ca. 1930 Ma with age peaks at 1611 and 1763 Ma (Fig. 3A–F). Inherited grains yield a dominant Neoproterozoic–Cambrian population with some older and younger ages (Fig. 3G).

**Ford Granodiorite suite, granites and diatexites**

Representative cathodoluminescence (CL) images of zircons from six Ford Granodiorite suite samples, two diatexite samples and one Upper Devonian granite dated in this study are shown in Figure 4. U–Pb results are reported in Tables DR4–5, plotted on U–Pb Tera–Wasserberg concordia diagrams and as probability distributions (with stacked histograms) in Figure 5. Final ages are summarized in Table 2; these ages are interpreted to date crystallization with the exception of the diatexite (Y1-IG071). For this sample, no statistically significant age was obtained.

## MAJOR OXIDE AND TRACE ELEMENT GEOCHEMISTRY

The geochemistry of the samples from this study (supplementary table DR2), combined with geochemical data from Korhonen et al. (2010a) and Weaver et al. (1991, 1992), Pankhurst et al. (1998) and Tulloch et al. (2009) for 15 Ford Granodiorite suite samples, is plotted as a series of Harker diagrams in Figure 6. Normalized rare earth element (REE) patterns are given in Figure 7.

### *Swanson Formation*

The Swanson Formation has $SiO_2$ contents ranging from 61 to 74 wt % (Fig. 6); although variable, individual samples are peraluminous with aluminum saturation indices (ASI= Molar [$Al_2O_3$/(CaO+$Na_2O$+$K_2O$)]) of 1.2–2.0, decreasing with increasing $SiO_2$. With increasing $SiO_2$, $TiO_2$, CaO, $Na_2O$, U, Th, Sr, Ba and La remain relatively constant, whereas $Al_2O_3$, $K_2O$, FeO*+MgO, Rb and Rb/Sr decrease, and Zr increases (Fig. 6). The Swanson Formation has limited variation in REE abundances; individual samples are characterized by normalized patterns (Fig. 7) that are smooth for the LREE and flat for the HREE, with consistent $La_N/Lu_N$ of 8–11 and moderate negative Eu anomalies ($Eu_N/Eu_N^*$ = 0.6–0.7).

*Ford Granodiorite suite*

The Ford Granodiorite suite has $SiO_2$ contents ranging from 64 to 76 wt % (Fig. 6); individual samples vary from metaluminous to peraluminous with increasing $SiO_2$ (ASI = 0.9–1.2). With increasing $SiO_2$, $K_2O$ and Th increase, and although Rb, Sr and Rb/Sr are variable at $SiO_2$ <71 wt %, at $SiO_2$ >71 wt % Rb increases, Sr decreases and Rb/Sr increases (Fig. 6). By contrast, $Al_2O_3$, CaO, FeO*+MgO, $TiO_2$, Zr, and Ba decrease, whereas $Na_2O$ and La remain relatively constant and U is highly variable (Fig. 6). The Ford Granodiorite suite has a wider range of REE abundances than the Swanson Formation; individual samples have mostly smooth LREE patterns and smooth to concave up HREE (Gd–Lu) patterns (Fig. 7), with $La_N/Lu_N$ of 6–15 and variable negative Eu anomalies ($Eu_N/Eu_N^*$ = 0.3–0.8).

*Devonian–Carboniferous granites and diatexites*

Devonian–Carboniferous granites have $SiO_2$ contents ranging from 65 to 72 wt % (Fig. 6); they are metaluminous to peraluminous (ASI = 1.0–1.2). Although the geochemistry is variable with increasing $SiO_2$, the granites show decreasing $Al_2O_3$, CaO, FeO*+MgO, $TiO_2$, Zr and Ba, whereas $K_2O$, U, Th, Rb Sr, Rb/Sr and La show no trend and $Na_2O$ increases (Fig. 6). The granites have elevated LREE and depressed HREE relative to the Ford Granodiorite suite; individual samples have smooth LREE patterns and smooth to concave up HREE patterns (Fig. 7), with $La_N/Lu_N$ of 12–77 and variable negative Eu anomalies ($Eu_N/Eu_N^*$ = 0.4–0.8).

The two diatexites have $SiO_2$ of 72 and 73 wt%; they are both peraluminous (ASI = 1.1 and 1.2) with Rb/Sr ratios <1. Sample Y1-IG073 has higher Zr, Th, Ba and La, but otherwise the major oxides and other trace element abundances are comparable to each other (Fig. 6). The diatexites have steep chondrite-normalized REE patterns ($La_N/Lu_N$ = 55 and 22) with elevated LREE and depressed HREE relative to the Ford Granodiorite suite and negative Eu anomalies ($Eu_N/Eu_N^*$ = 0.5 and 0.6) similar to those of the granites (Fig. 7).

**Sr and Sm–Nd RESULTS**

Newly analyzed samples of the Swanson Formation have $^{87}Sr/^{86}Sr_{360Ma}$ values of 0.7119–0.7204 and $\varepsilon Nd_{360Ma}$ values that range from -9.3 to -6.3 (Fig. 8), whereas newly analyzed samples of the Ford Granodiorite suite have $^{87}Sr/^{86}Sr_{360Ma}$ values of 0.7052–0.7092 and $\varepsilon Nd_{360Ma}$ values that range from -3.1 to -0.2 (Fig. 8). Two newly analyzed Devonian–Carboniferous granites (Y1-AE035 and M5-G175) have $^{87}Sr/^{86}Sr_{360Ma}$ values of 0.7075 and 0.7091, and $\varepsilon Nd_{360Ma}$ values of -4.3 and -3.8, respectively (Fig. 8). A homogenous diatexite (Y1-IG073) has $^{87}Sr/^{86}Sr_{360Ma}$ of 0.7094 and a $\varepsilon Nd_{360Ma}$ value of -4.3 (Fig. 8), whereas an inhomogeneous diatexite (Y1-IG071) has $^{87}Sr/^{86}Sr_{360Ma}$ of 0.7045 and a $\varepsilon Nd_{360Ma}$ value of -5.7 (Fig. 8).

**Hf AND O RESULTS**

**Swanson Formation and calc-silicate gneiss**

U–Pb, Hf and O data from detrital zircons are plotted in Figure 9. Detrital zircons from sample Y2-MP098 yielded $\varepsilon Hf_t$ ($\varepsilon$Hf calculated at the U–Pb age) values that range from -24.5 to 9.7 (Fig. 9A) and roughly half are negative (26 of 45). Sample Y2-MD092 contains detrital zircons with $\varepsilon Hf_t$ values that range from -13.4 to 8.2 (Fig. 9A), and again approximately half are negative (25 of 49).

Detrital zircons from sample 8D27-10 (calc-silicate gneiss) define the same U–Pb age populations as samples of the Swanson Formation. Therefore, published data for this sample (Yakymchuk et al., 2013a) have been included in the final data set for the Swanson Formation discussed below. This sample has $\varepsilon Hf_t$ values that mostly range from -3.7 to +6.0, with two outlying values of -11.4 and +8.9 (Fig. 9A; Yakymchuk et al., 2013a). The range of $\delta^{18}O$ values for detrital zircons from the calc-silicate gneiss (8D27-10) is from 6.4 to 10.8 ‰, with one value of 16.6 ‰ (Fig. 9B; Yakymchuk et al., 2013a). Zircons from the Neoproterozoic–Cambrian and Mesoproterozoic populations both have a similar range of $\delta^{18}O$ values that are between those expected for zircon crystallized from juvenile magmas and those derived solely from a supracrustal source (Fig. 9B).

Combining data from the three samples yields a range of $\varepsilon Hf_t$ values for each of the three age populations, as follows. For the Neoproterozoic–Cambrian population, $\varepsilon Hf_t$ values mostly lie between -10 and +3, whereas for the Mesoproterozoic population, most $\varepsilon Hf_t$ values range from +1 to +10. For the Paleoproterozoic population, $\varepsilon Hf_t$ values vary from -7 to +7, but most are negative with one value of -17, and, Archean grains have only negative $\varepsilon Hf_t$ values that range from -6.1 to -0.4.

For whole-rock oxygen isotope analysis, six of the eight analyzed Swanson Formation samples yielded whole-rock $\delta^{18}O$ oxygen values that range from +10.0 to +13.5, which give an average value of +11.9 (GSA Data Repository). Two samples (10CY-001 and 10CY-002) are metasedimentary hornfels collected from the contact aureole of a Cretaceous pluton in the Clark Mountains; these samples yielded whole-rock $\delta^{18}O$ values of -6.9 and -9.2, respectively.

**Ford Granodiorite suite and diatexite**

The individual Hf and O results vs. crystallization age for zircons from the Ford Granodiorite suite and diatexite samples from this study are summarized in Figure 10. Zircons from sample Y2-JU096 have $\varepsilon Hf_t$ values that range from -4.4 to +1.7, and $\delta^{18}O$ values that vary from 7.4 to 9.6, with weighted means of -1.6 ± 1.1 and 8.8 ± 0.3, respectively ( σ ; 13 of 18). Zircons from sample 51225-2 have $\varepsilon Hf_t$ values that range from -4.5 to +0.4 (with two values of -8.6 and -9.5), and $\delta^{18}O$ values that vary from 8.4 to 10.5 (with two values of 4.6 and 7.5), with weighted means of -2.1 ± 1.0 and 9.5 ± 0.3, respectively ( σ ; 15 of 17). Zircons from sample 9N27-4 have $\varepsilon Hf_t$ values that range from -5.3 to +0.2, and $\delta^{18}O$ values that vary from 7.0 to 9.7, with weighted means of -3.3 ± 1.0 and 7.6 ± 0.3, respectively ( σ ; 13 of 15). Zircons from sample 912-2A have $\varepsilon Hf_t$ values that range from -4.8 to +1.9 (with one value of -13.8), and $\delta^{18}O$ values that vary from 8.0 to 9.3 (with one value of 7.4), with weighted means of -1.9 ± 0.8 and 8.7 ± 0.2, respectively ( σ ; 14 of 15).

The inhomogeneous diatexite (Y1-IG071) yields a wide range of U–Pb ages with two dominant populations: Upper Devonian and Cretaceous (Fig. 5). Zircons from the older population have $\varepsilon Hf_{360}$ values of -9.8 to -1.3, and $\delta^{18}O$ values of 9.4 to 10.6, with weighted means of -6.9 ± 2.7 and 10.0 ± 0.6, respectively ( σ ; n = 6). Zircons from the younger population have $\varepsilon Hf_{100}$ values of -10.0 to -4.7 (one value of -13.5), and $\delta^{18}O$ values of 9.5 to 10.2 (one value of 4.7), with weighted means of -7.2 ± 1.2 and 9.8 ± 0.2, respectively ( σ ; 9 of 10). The homogenous diatexite (Y1-IG073) contains only Upper Devonian zircons that have $\varepsilon Hf_t$ values of -3.9 to -2.1, and $\delta^{18}O$ values of 8.5 to 10.4, with weighted means of -3.1 ± 0.3 and 9.6 ± 0.2, respectively ( σ ; 18 of 19).

## DISCUSSION

### Possible sources for the Swanson Formation detrital zircons

The U–Pb ages and $\varepsilon Hf_t$ values from detrital zircons may be used to assess potential sources for each zircon population identified in the Swanson Formation samples, as discussed below. The plausibility of these potential source materials based on U–Pb ages and $\varepsilon Hf_t$ values is evaluated using a $\varepsilon Hf_t$ evolution plot in Figure 11.

Paleoproterozoic (ca. 1.7 Ga) zircons from the Swanson Formation have $\varepsilon Hf_t$ values that range from -7 to +7, with one value of -17 (Fig. 11). The Nimrod Group, which crops out in the Miller Range of central Transantarctic Mountains (Fig. 1A), includes rocks with zircon of the same age range (Goodge and Fanning, 2002). Igneous zircons from Archean layered gneisses in the Nimrod Group have metamorphic overgrowths dated at 1730–1720 Ma. In addition, a single deformed granodiorite yielded a crystallization age of ca. 1730 Ma (Goodge et al., 2001). This exposure of Precambrian basement in the central Transantarctic Mountains, which is inferred to continue under the ice (Goodge and Finn, 2010), represents a possible source for the Paleoproterozoic and older zircons in the Swanson Formation samples.

Most Mesoproterozoic zircons in the Swanson Formation have positive $\varepsilon Hf_t$ values, suggesting a relatively juvenile source. The gneiss at Haag Nunataks, located to the northeast of the Ellsworth Mountains (Flowerdew et al., 2007), is the only exposure of probable Mesoproterozoic basement in West Antarctica. An Rb–Sr whole-rock isochron age of 1176 ± 76 Ma was interpreted to date crystallization of the protolith of this gneiss (Millar and Pankhurst, 1987). Slightly younger Rb–Sr whole-rock isochron ages were obtained from cross cutting microgranite (1058 ± 53 Ma) and aplogranite and pegmatite (1003 ± 18 Ma) from this outcrop (Millar and Pankhurst, 1987). For the gneiss, $\varepsilon Hf_t$ values from zircon range from +6.7 to +9.2

(Flowerdew et al., 2007) and whole-rock Nd isotope analysis yielded a depleted mantle model age of ca. 1250 Ma (Storey et al., 1994). Taken together, these data suggest that the gneiss at Haag Nunataks represents a relatively juvenile addition to the crust during the Mesoproterozoic, qualifying it as a potential source for this population of detrital zircons.

Other possible sources for Mesoproterozoic detrital zircons in the Swanson Formation lie beneath the Antarctic ice sheet. For example, Tochilin et al. (2012) report detrital zircon U–Pb age populations of 512–540 Ma and 800–1100 Ma from Oligocene–Quaternary sedimentary rocks in drill core from the Prydz Bay region (Fig. 1A), which is estimated to drain roughly 16% of the East Antarctica Ice Sheet. In addition, direct samples of the bedrock beneath the Antarctic ice sheet are provided by clasts from glacial moraines (e.g. Goodge et al., 2010, 2012). Zircons from granite clasts in Quaternary glacial tills in the Central Transantarctic Mountains yielded $\varepsilon Hf_t$ values of +2 to +6 at ca. 1.2 Ga (Goodge et al., 2013). These clasts suggest the presence of a Mesoproterozoic orogenic belt under the ice inland from the Transantarctic Mountains that has been speculatively linked to the Gamburtsev Subglacial Mountains and the Vostok Subglacial Highlands of East Antarctica (e.g. Elliot et al., 2014).

The Mesoproterozoic population of detrital zircons from the Swanson Formation, with the exception of three grains, is younger than both the gneiss at Haag Nunataks (based on the 1176 ± 76 Ma Rb–Sr isochron age of the gneiss) and the ca. 1.2 Ga granite clast from the Central Transantarctic Mountains (Fig. 11). However, for an average crustal $^{176}Lu/^{177}Hf$ ratio (Vervoort and Patchett, 1996; Vervoort et al., 1999), within $\pm 1\sigma$ uncertainty, the $\varepsilon Hf$ evolution lines from these potential sources enclose most of the Mesoproterozoic detrital zircon data from the Swanson Formation samples. This permits the Mesoproterozoic zircons to have been derived from source materials similar to these examples.

Mesoproterozoic zircons from sample 8D27-10 yielded $\delta^{18}O$ values above those expected for juvenile material derived directly from the mantle (Fig. 9B), which indicates the involvement of a supracrustal component. This is consistent with crustal reworking during a Mesoproterozoic orogenic event. If these zircon grains were derived from rocks inland of the Transantarctic mountains, which seems likely, the $\delta^{18}O$ values of the zircons lends support to the existence of Grenville-age orogenic belt exposed beneath the East Antarctic Ice sheet (e.g. Goodge et al., 2010; Elliot et al., 2014).

The Neoproterozoic–Cambrian population of zircons from the Swanson Formation contains more evolved $\varepsilon Hf_t$ values than the Mesoproterozoic population, which is consistent with derivation from igneous and metamorphic rocks associated with crustal reworking in the Ross–Delamerian orogen (Ireland et al., 1998; Adams et al., 2013). In the central Transantarctic Mountains, the oldest intrusive rocks are dated at ca. 550 Ma (Rowell et al., 1993) and widespread magmatism associated with the Ross Orogen is dated at 520–480 Ma (Goodge et al., 2012; Paulsen et al., 2013). In the Wilson Terrane of north Victoria Land, the Granite Harbour Intrusives have been dated at 520–490 Ma (Borg et al., 1986; Vetter et al., 1987; Dallai et al., 2003; Goodge et al., 2012). Although there are no reported εHf values for these rocks, some diorites, granites and granodiorites have $\delta^{18}O$ values consistent with a significant crustal component (Dallai et al., 2003). In the Dry Valleys of south Victoria Land, a minor episode of magmatism at 530–505 Ma was followed by the emplacement of a large volume of calc-alkaline granite at 505–500 Ma (Allibone and Wysoczanski, 2002). However, most zircons from the Neoproterozoic–Cambrian population from the Swanson Formation are older than most igneous and metamorphic rocks reported from the Ross Orogen as described above. Evidence of an older potential source comes from the Central Transantarctic Mountains where glacial clasts in moraines are inferred to be samples of the subglacial bedrock. These rocks have U–Pb zircon ages of 590–490 Ma (Goodge et al., 2012).

Most ages from the Neoproterozoic–Cambrian population of zircons from the Swanson Formation are older than most of igneous rocks from north Victoria Land and the Transantarctic Mountains, with the exception of a ca. 590 Ma glacial clast reported in Goodge et al. (2012). However, most of the Neoproterozoic–Cambrian zircons from the Swanson Formation plot along the same εHf evolution lines as the Mesoproterozoic population of detrital zircons discussed above (Fig. 11). This suggests that most of the detrital zircons in the Swanson Formation could have been derived from crust, or sedimentary derivatives of crust, that is similar to the gneiss at Haag Nunataks and the ca 1.2 Ga Mesoproterozoic granite clasts that originated from beneath the East Antarctic ice sheet.

**Detrital zircon provenance across the former margin of East Gondwana**

The three age populations of detrital zircons from the Swanson Formation are broadly consistent with the provenance of Early Paleozoic sediments along the eastern portion of Gondwanan margin, which extended from Australia through West Antarctica and the Antarctic Peninsula into South America (Ireland et al., 1998; Adams et al., 2005; Adams, 2010; Adams et al., 2013). In particular, the detrital zircon patterns of the Swanson Formation are similar to those from the Lachlan Group in eastern Australia, the Robertson Bay Group in North Victoria Land, and the Greenland Group in the Western Province of New Zealand (Ireland et al., 1998; Adams et al., 2013). The maximum depositional ages and the youngest zircon ages are similar for these three groups and the Swanson Formation. In addition, the U–Pb age distributions of detrital zircons from the Swanson Formation are similar to those from metasedimentary rocks from the

Trinity Peninsula Group and Fitzgerald Quartzite on the Antarctic Peninsula (Flowerdew et al., 2006a; Bradshaw et al., 2012), sedimentary rocks from the Ellsworth–Whitmore Mountains (Flowerdew et al., 2007) and Ross supergroup sandstones in the Queen Maud Mountains (Paulsen et al., 2015).

In general, the $\varepsilon Hf_t$ values of Neoproterozoic–Cambrian and Mesoproterozoic populations of zircons from sedimentary rocks deposited along the East Gondwana margin are similar to those from the Swanson Formation. For example, the Trinity Peninsula Group on the Antarctic Peninsula has detrital zircon age populations of 1100–1000 Ma and 620–500 Ma for which the majority of $\varepsilon Hf_t$ values from each group range from +2 to +12 and -8 to +2, respectively (Bradshaw et al., 2012). Flowerdew et al. (2006a) report juvenile Hf isotope values from older zircon populations and less radiogenic Hf isotope values from the dominant (ca. 540 Ma) zircon population in the Fitzgerald Quartzite. Neoproterozoic–Cambrian zircons from the Greenland Group in New Zealand yield $\varepsilon Hf_t$ values of -20 to +8 (Nebel-Jacobsen et al., 2011). Detrital zircon in paragneisses from the Western Province of New Zealand show a similar distribution of ages to the Swanson Formation and yield $\varepsilon Hf_t$ and $\delta^{18}O$ values that indicate an increase in the amount of crustal reworking through time (Hiess et al., 2014). Ordovician volcaniclastic rocks deposited on the margin of the Macquarie Arc in the Tasmanides also show negative $\varepsilon Hf_t$ values for Neoproterozoic–Cambrian zircons and slightly negative to positive values for 1250–970 Ma detrital zircons (Glen et al., 2011).

The similarity of U–Pb ages and $\varepsilon Hf_t$ values of detrital zircons from Cambrian–Ordovician sedimentary rocks deposited across the East Gondwana margin suggest a laterally extensive source region. Neoproterozoic–Cambrian zircons reflect predominantly crustal reworking and likely originated from the Ross–Delamerian orogen and its putative inland extension beneath the Antarctic ice sheet. The location of an extensive source of relatively juvenile Mesoproterozoic material is more problematic, but the Grenville-age orogenic belt hypothesized to occur beneath the East Antarctic ice sheet is a possible solution.

**$\delta^{18}$O values of the Swanson Formation**

Sedimentary rocks and granites derived from them can be distinguished from granites with juvenile sources using oxygen isotopes (e g O'Neil and Chappell, 1977). To evaluate the proportional contribution of the Swanson Formation to the petrogenesis of granites in western Marie Byrd Land it is necessary to know the $\varepsilon Hf_t$ values of the detrital zircon and the $\delta^{18}$O values of whole-rock samples. For six of the eight samples of Swanson Formation, whole-rock values range from 10.0 to 13.5‰, which are similar to values expected for most sedimentary rocks (~12‰; O'Neil and Chappell 1977). However, these values are lower than whole-rock values reported for the correlative Greenland Group of 13.7–16.2‰ (Tulloch et al , 009) used by Yakymchuk et al. (2013a) to model mixing of material between the Ford Granodiorite suite and the Swanson Formation. During partial melting, oxygen isotope fractionation between zircon and granitic magma will result in igneous zircons that have $\delta^{18}$O values less than the source rock by 1–2‰ (Valley et al , 1994; Valley, 2003). Therefore, using a $\Delta^{18}O_{Zrc-WR}$ correction of -1 5‰ for isotope fractionation, newly crystallized zircons in granites derived from partial melting of the Swanson Formation are predicted to have a $\delta^{18}$O values of ~8.5–12‰.

Two Swanson Formation samples from the contact aureole around a Cretaceous pluton show negative whole-rock $\delta^{18}$O values of -6.9 and -9.2‰ (GSA Data Repository Table DR7). Negative values are consistent with hydrothermal alteration associated with an active magma chamber at a shallow enough depth to allow the penetration of negative $\delta^{18}$O meteoric water. A strong isotope exchange between the rocks and meteoric water is needed to produce the negative isotope values observed in these two samples. Furthermore, the strongly negative $\delta^{18}O$ values of the meteoric water necessary for hydrothermal alteration of these two Swanson Formation samples are compatible with high latitudes, consistent with the position of western Marie Byrd Land during the Cretaceous (e.g. DiVenere et al., 1994).

**Petrogenesis of the Ford Granodiorite suite, the granites and the diatexites**

*Temporal changes in Hf and O isotopes in zircon*

For a fuller assessment of the relationships among the Ford Granodiorite suite, the granites and the diatexites, and due consideration of their petrogenesis, the six new Hf and O isotope datasets reported in this study have been combined with published information for four additional samples (from Yakymchuk et al., 2013a; Ford Granodiorite suite samples MB.214.W and MB.219.W, and granite samples M5-G175 and C5-Is51A). The combined dataset is shown as ten box-and-whisker plots for $\varepsilon Hf_t$ and $\delta^{18}O$ vs. age in Figure 12. Box-and-whisker plots are used because the data are not normally distributed. These plots provide a graphical summary of dataset characteristics based on percentile rank analysis and plotting the maximum and minimum dataset values. Importantly, the underlying statistics are less sensitive toward individual outliers than other methods of analysis (Tukey, 1977). Also, the compact nature of the plots allows side-by-side comparison of individual sample datasets. Nonparametric statistics may be used to evaluate whether the distributions of zircon $\varepsilon Hf_t$ and $\delta^{18}O$ values are significantly different between samples of the Ford Granodiorite suite, and between these and the granites and diatexites. We use the nonparametric Kruskal–Wallis test (Kruskal and Wallis, 1952) that is analogous to a parametric analysis of variances (ANOVA) test, except that it does not require data that are normally distributed.

The Ford Granodiorite suite samples divide into two groups. The two oldest members of the suite (MB.214 and MB.219) have zircon with the most radiogenic $\varepsilon Hf_t$ and the lowest $\delta^{18}O$ values, whereas the four younger samples have zircons with more evolved $\varepsilon Hf_t$ and higher $\delta^{18}O$ values (Fig. 12). Based on results from the Kruskal–Wallis test (supplementary table DR10), samples within each group are likely to have sampled the same population, whereas the two groups of samples are likely to have sampled different populations. The $\varepsilon Hf_t$ and $\delta^{18}O$ values for the granites and diatexites are similar to the younger group of Ford Granodiorite suite samples (Fig. 12, supplementary table DR10). These data suggest a change at ca. 370 Ma towards a larger contribution from the Swanson Formation in the petrogenesis of the younger rocks. This change is consistent with the study of Tulloch et al. (2009), who reported monazite $^{207}Pb/^{235}U$ ages of ca. 359 Ma and ca. 351 Ma from muscovite–biotite granites from the Chester Mountains and Neptune Nunataks (locations in Fig. 2), respectively, consistent with the postulated increasing contribution from a sedimentary source after ca. 370 Ma.

*Potential source rocks*

Zircons from the Ford Granodiorite suite, the Devonian–Carboniferous granites and the diatexites exhibit a range of $\delta^{18}O$ and $\varepsilon Hf_t$ values. Many arc-related granitoids are thought to represent a mixture of two or more source components (e.g. Kemp et al., 2009; Miles et al., 2014). The Hf and O isotope composition of zircon provides a potentially powerful tool to evaluate the nature and proportional contribution of these source components to granitoid petrogenesis (e.g. Kemp et al., 2007). These proportions may be evaluated if the isotope composition of the source components is known and if they are sufficiently distinct from one another. Hf isotopes may be used to distinguish between juvenile and ancient source components, whereas O isotopes may be used to determine if source components have been subjected to surface processes, such as weathering and sedimentation, as indicated by high $\delta^{18}O$ values (e.g. Hawkesworth and Kemp, 2006).

The majority of Hf in most crustal rocks is found in zircon. In a closed system, zircon dissolution during partial melting will contribute Hf to the melt, which partitions into newly formed zircon during melt crystallization. In this scenario, newly formed zircon is predicted to have a similar Hf isotope composition to that of zircon in the protolith (e.g. Flowerdew et al., 2006b). Although the breakdown of high Lu/Hf minerals such as apatite may also contribute radiogenic Hf to the melt, the amount of Hf is expected to be relatively minor compared with Hf contribution from the breakdown of zircon. Therefore, in a closed system, newly formed zircon in a crystallized anatectic melt is predicted to have a similar Hf isotope composition to the original magmatic grains in an igneous protolith, or to the detrital zircons in a metasedimentary protolith, or to an intermediate composition where derived from a mixed source.

Oxygen isotope fractionation between zircon and granite magma will result in igneous zircons that have slightly lower $\delta^{18}O$ values (Valley et al., 1994; Valley 2003). By contrast, the $\delta^{18}O$ composition measured in detrital zircon may not be representative of the whole-rock value because oxygen is a major component in all of the major rock forming minerals, including those that have formed at or near the surface. Therefore, granites derived by anatexis from sedimentary protoliths may not have similar oxygen isotope compositions to detrital zircons in the source, but they are expected have a composition similar to the whole rocks.

For the Ford Granodiorite suite, one potential source component is the regionally distributed Swanson Formation. The εHf values of detrital zircons in the Swanson Formation, recalculated to 360 Ma, vary from +2 to -67, with a median value of -11.7 and an interquartile range of -3.5 to -19.9 (Figs. 10, 12 and 13). As discussed above, the $\delta^{18}O$ value of zircons that crystallized from melt produced from the Swanson Formation are expected to have values of ~8.5–12‰, with a mean value of 10.5‰ (Figs. 10, 12 and 13). The Hf isotope composition of zircons from the Ford Granodiorite suite reported in this study is more radiogenic than most detrital zircons from the Swanson Formation (Fig. 10A). This suggests the involvement of a source more juvenile than the Swanson Formation.

The calc-alkaline chemistry of the Ford Granodiorite suite and its emplacement during a period of widespread arc magmatism along the East Gondwanan plate margin suggests the possible involvement of juvenile magma sourced from the arc mantle or a mafic underplate derived from it. Such a source is inferred to have a $\delta^{18}O$ value of 5.3 ± 0.6‰ (Valley et al., 1998). The εHf of this source may range from that expected for new crust sourced from a slightly enriched mantle wedge in an island arc (+12.2 at 360 Ma; Dhuime et al., 2011) to less radiogenic values associated with a more enriched sub-continental lithospheric mantle above a subducting slab. The εHf values for modified sub-continental lithospheric mantle may range from 0 (CHUR) to +10 (Griffin et al., 2000). Therefore, for the purpose of petrogenetic modeling, two end-member εHf values of 0 (CHUR) and +12.2 (new crust) have been chosen to represent the juvenile source.

Excluding outliers (Fig. 12), data from the Ford Granodiorite suite reported in this study have $\varepsilon Hf_t$ values that plot between those for the Swanson Formation and those for the juvenile source (Fig. 10A). This suggests that a petrogenetic scenario similar to the model developed for granites in the Lachlan Fold Belt of the Tasmanides orogen may be applicable to the Ford Granodiorite suite. The Lachlan granites were interpreted to be the mixed products of sedimentary material reworked by juvenile magma in the deep crust (Kemp et al., 2007).

Accordingly, binary mixing curves between Swanson Formation and mantle have been calculated to evaluate this model for the petrogenesis of the Ford Granodiorite suite (Fig. 13A). Four scenarios are modeled: two where different juvenile magma compositions, discussed above, are mixed with Swanson Formation *en masse* and two where these same juvenile magma compositions are mixed with anatectic melt derived from the Swanson Formation.

The curvature of the mixing lines is most sensitive to the relative concentrations of Hf in each of the end-members. There are no data available for mafic rocks of an appropriate age in Marie Byrd Land. Therefore, for the juvenile source, an Hf concentration of 2.3 ppm is used, which is a representative composition for mafic rocks temporally associated with Devonian granites in the Lachlan Fold Belt of the Tasmanides orogen (e.g. Kemp et al., 2007). For the Swanson Formation, an average whole-rock concentration of 3.2 ppm was assigned based on bulk chemical analyses (Korhonen et al., 2010a). For melt derived from the Swanson Formation, a concentration of 1.0 ppm is used, which represents the average Hf concentration of deep crustal granites that were interpreted to be derived predominantly from a Swanson Formation source inside the Fosdick complex (Korhonen et al., 2010a).

For the four younger Ford Granodiorite suite samples analyzed in this study, a large proportion of the Hf and O isotope compositions of the zircons may be explained by this model, particularly for mixing magma from the juvenile source with anatectic melt from the Swanson Formation. This is consistent with rare zircon cores within some samples that correspond to the main age populations found in the Swanson Formation and paragneiss detrital zircons (Fig. 3). Mixing between juvenile magma and 40–80% anatectic melt derived from the Swanson Formation is required to explain the range of measured values for the Ford Granodiorite suite samples (Fig. 13A).

An alternative scenario that cannot be ruled out by the data is one in which the earliest members of the Ford Granodiorite suite are reworked in the deep crust, generating melts that mix with those derived from the Swanson Formation or assimilate Swanson Formation *en masse* to produce the younger members of the Ford Granodiorite suite. To explore this scenario the data from this study are combined with data from Yakymchuk et al. (2013a). These data are plotted as two fields in Figure 13B, one for two older members of the Ford Granodiorite suite (samples MB.214 and MB.219) and a second for the four younger members of the Ford Granodiorite suite shown in Figure 13A. Most of the Hf and O isotope compositions of zircons from the younger members of the Ford Granodiorite suite may be explained by mixing of anatectic melt from older members of the suite with anatectic melt from the Swanson Formation (Fig. 13B). This is consistent with the small population of slightly older zircon dates from sample Y2-JU096 that yielded an age of ca. 377 Ma (Fig. 5). However, the Hf and O isotope composition of zircons from samples MB.214 and MB.219 also lie inside the curves for juvenile magma mixing with melts derived from the Swanson Formation or for assimilation of Swanson Formation *en masse* (compare the fields in Fig. 13B with the model mixing curves in Fig. 13A). Thus, any contribution to the petrogenesis of the younger members of the Ford Granodiorite suite derived by reworking of these older compositions would have been masked by any ongoing input from the juvenile mantle source, and the two alternative scenarios cannot be distinguished.

*The granites and diatexites*

The granites and diatexites generally have whole-rock Sr and Nd, and zircon Hf and O isotope compositions that lie between those of the most primitive Ford Granodiorite suite members and the least evolved Swanson Formation (Figs. 6 and 13). This observation permits a variety of plausible scenarios for the petrogenesis of the granites and diatexites.

The first possibility is that juvenile magma could have assimilated Swanson Formation *en masse* or mixed with anatectic melt derived from the Swanson Formation in a fashion similar to the model proposed for the petrogenesis of the Ford Granodiorite suite (compare the data in Fig. 13C with the model mixing curves in Fig. 13A). However, this option considered the least likely based on the variable oxide and trace element distributions of the granites and diatexites compared with the more regular distributions shown by the Ford Granodiorite suite samples (Fig. 6) and the differences in REE patterns (Fig. 7).

Four alternative possibilities are: (1) Ford Granodiorite suite magmas could have mixed with anatectic melt derived from the Swanson Formation, (2) Ford Granodiorite suite magmas could have assimilated Swanson Formation *en masse*, (3) melt derived from early-crystallized members of the Ford Granodiorite suite by anatexis could have mixed with anatectic melt derived from the Swanson Formation, and (4) melt derived from early-crystallized members of the Ford Granodiorite suite by anatexis could have assimilated Swanson Formation *en masse*, as proposed by Korhonen et al. (2010a).

First, we evaluate these four options using the Sr and Nd isotope compositions recalculated to 360 Ma. Figure 8 shows binary mixing lines that connect representative compositions of the Swanson Formation and the Ford Granodiorite suite calculated using the Sr and Nd concentrations and isotope values of more and less radiogenic end-member samples (Fig. 8). With the exception of granite sample C5-Is51a (reported by Korhonen et al., 2010a) and the inhomogeneous diatexite (Y1-IG071), the granites plot between the two sources but closer to the Ford Granodiorite suite. The Sr and Nd isotope values of the granites and the homogeneous diatexite allow a contribution of up to 30 vol.% Swanson Formation (Fig. 8). The inhomogeneous diatexite (Y1-IG071) plots at less radiogenic εNd values than the Ford Granodiorite suite but also at lower $^{87}Sr/^{86}Sr_{360}$ values than the Swanson Formation (Fig. 8). This sample contains a significant population of 100 Ma zircons. If the Sr and Nd isotope ratios are recalculated to 100 Ma, the inhomogeneous diatexite falls between the εNd and $^{87}Sr/^{86}Sr_{100}$ values of two putative sources, which is interpreted to indicate that this sample records the effects of the Cretaceous overprint in the Fosdick complex.

Second, we use the zircon Hf and O isotope compositions. Figure 13C shows binary mixing lines that connect representative compositions of the Swanson Formation and the Ford Granodiorite suite. These were calculated using Hf concentrations of 3.3 ppm for the Ford Granodiorite suite magmas and 1.0 ppm for anatectic melts derived from early members of the Ford Granodiorite suite combined with the Hf concentrations discussed above for the Swanson Formation. Note that assimilation of Swanson Formation *en masse* by Ford Granodiorite suite magma and mixing of anatectic melts derived from early members of the Ford Granodiorite suite with those derived from the Swanson Formation yield similar binary mixing curves that cannot be distinguished in Figure 13C. The modeling permits by all four petrogenetic scenarios discussed above; in almost all cases the proportion of Ford Granodiorite suite component required by the data is greater than the Swanson Formation component.

To further test these two alternatives, the major-element compositional variability of Devonian–Carboniferous granites and diatexites is investigated using the ternary system (Na+Ca)–(Fe*+Mg+Ti)–K (Solar and Brown, 2001). Because there have been no melting experiments done on the either the Ford Granodiorite suite or the Swanson Formation, experimental melt compositions from Skjerlie et al. (1993) and Patiño Douce and Harris (1998) were used based on similarity in chemical composition of the experimental starting materials to the putative sources of the granites. The experimental melts from Skjerlie et al. (1993) were used as proxies for melts derived from the Ford Granodiorite suite while the experimental results of Patiño Douce and Harris (1998) were used to infer melt compositions derived from the Swanson Formation. The compositions of the starting materials and melts are plotted along with samples from the Swanson Formation, Ford Granodiorite suite, and the granites and diatexites in Figure 14. There is a wide range of possible granite and diatexite compositions that may be achieved by assimilation or mixing between Ford Granodiorite suite compositions, Swanson Formation compositions and melts derived from each, as shown by the shaded areas in Figure 14, particularly given the propensity of crustal melts to entrain peritectic residue (Clemens et al., 2011; Clemens and Stevens, 2012). As a result, the four alternative petrogenetic scenarios considered—that Ford Granodiorite suite magmas or melts derived from early-crystallized members of the suite could have assimilated Swanson Formation *en masse* or mixed with anatectic melt derived from the Swanson Formation—cannot be discriminated.

## WIDER CONSIDERATIONS

### Implications for a Proterozoic basement

An outstanding question in western Marie Byrd Land is the nature and age of the basement to the Swanson Formation. Evidence supporting a Proterozoic basement includes: (1) inherited zircons in granites that yield Proterozoic ages (Fig. 3G) or Proterozoic concordia upper intercept ages (Pankhurst et al., 1998; Mukasa and Dalziel, 2000); (2) Proterozoic Nd model ages for the Ford Granodiorite suite (Pankhurst et al., 1998); and (3) Proterozoic Os isotope model ages for peridotite xenoliths from the upper mantle beneath Eastern Marie Byrd Land, which assumes that the crust and underlying mantle are temporally coupled (Handler et al., 2003). However, aeromagnetic anomalies north Victoria Land led Finn et al. (1999) to suggest that sedimentary rocks that make up the Robertson Bay Terrane—proposed to be correlative with the Swanson Formation in Marie Byrd Land—were deposited on forearc oceanic crust. The geological and geochemical evidence for the age of the basement to the Swanson Formation is evaluated below.

Granites from Marie Byrd Land commonly contain zircons with xenocrystic cores that may reflect inheritance from a Precambrian source (e.g. Mukasa and Dalziel, 2000), or alternatively, these grains may represent detrital zircons scavenged from sedimentary rocks during formation and/or emplacement. In the Ford Granodiorite suite, Devonian–Carboniferous granites and diatexites, inherited zircon grains yield dates of 2277 to 412 Ma and define a dominant Neoproterozoic–Cambrian population (Fig. 3G). The similarity of this age population to the Neoproterozoic–Cambrian age population in the Swanson Formation suggests the possibility of scavenged detrital zircon grains, which is supported by the requirement for a Swanson Formation component in the petrogenesis of the Ford Granodiorite suite, Devonian–Carboniferous granites and diatexites. Therefore, these inherited grains do not provide direct evidence of a Precambrian basement beneath western Marie Byrd Land.

The Ford Granodiorite suite yields Proterozoic Nd model ages that have been interpreted to reflect a Proterozoic basement in western Marie Byrd Land (Pankhurst et al., 1998). However, the Ford Granodiorite suite represents a mixture of juvenile (mantle-derived) and metasedimentary components, as demonstrated by the elevated $\delta^{18}O$ values of the zircons (Fig. 10). Therefore, the Nd model ages likely represent hybrids resulting from a mixture of two components and they may not reflect the true age of the basement.

Handler et al. (2003) document Mesoproterozoic Os model ages from mantle xenoliths in Cenozoic volcanic rocks from the Executive Committee Range in Marie Byrd Land, which is ~500 km away from the Ford Ranges. The partial melting and subsequent stabilization of mantle lithosphere at this time likely resulted in additions of juvenile magma to the crust, which potentially could represent a nearby source for Mesoproterozoic detrital zircons with juvenile $\varepsilon Hf_t$ values similar to those in the Swanson Formation. However, given the distance between the Ford Ranges and the Executive Committee Range, it is not required that the Swanson Formation was deposited on this Proterozoic basement.

An alternative model is that the Swanson Formation was deposited on a Paleozoic oceanic basement, as has been proposed for the Robertson Bay Terrane in north Victoria Land (Finn et al., 1999) and for the Lachlan Fold Belt of the Tasmanides orogen (Foster et al., 2009). A positive test of this hypothesis would be the retrieval of Paleozoic Os model ages from mantle xenoliths that occur in Cenozoic volcanic rocks in the Ford Ranges.

**Correlation along the Gondwana margin**

The former continental margin of Gondwana represents one of the most extensive and long-lived active convergent plate margins in the Phanerozoic and is the type example of an external (circum-Pacific) orogenic system (Cawood, 2005; Collins et al., 2011). Parts of the landmasses of Australia and New Zealand (Zealandia) were situated along the active margin of Gondwana together with north Victoria Land and Marie Byrd Land from the Paleozoic through the final breakup of Gondwana in the Cretaceous (Fig. 1B). The ages and isotope values of granites from different segments along the Gondwanan margin can provide insight into the similarities and differences in the processes operating along an active continental margin (e.g.

Yakymchuk et al., 2013a). However, such a comparison is limited by the paucity of zircon Hf isotope data from granites in New Zealand and north Victoria Land. Therefore, in this section we use both whole-rock Nd and zircon Hf isotope data from granites in each of these locations, as shown in Figure 15.

In eastern Australia, the Tasmanides orogen is attributed to alternating extensional and contractional tectonics associated with a west-dipping subduction zone that migrated oceanward from the Cambrian to the Permian (e.g. Collins, 2002; Glen, 2005; Cawood, 2005). A protracted period of Silurian to Devonian silicic magmatism is recorded in the Tasmanides with minor Carboniferous magmatism. These granites record a progression towards more radiogenic whole-rock εNd and zircon $\varepsilon Hf_t$ values with time (Fig. 15A, B), which has been tied to crustal growth accompanying slab rollback and back-arc rifting after crustal thickening (Kemp et al., 2009). Granites from the Western Province of New Zealand show a similar trend, although at a later time than the granites from the Tasmanides (Fig. 15A). In contrast, the Ford Granodiorite suite and its correlatives in north Victoria Land were emplaced over relatively short periods in the Devonian–Carboniferous and do not show the same temporal trends (Fig. 15A, B).

In north Victoria Land, correlative Devonian–Carboniferous igneous rocks include the Admiralty Intrusives (371–351 Ma; Borg et al., 1987; Fioretti et al. 1997; Henjes-Kunst and Kreuzer, 2003), the Salamander Granite complex (ca. 347 Ma; Henjes-Kunst and Kreuzer, 2003), and associated volcanic rocks (369–357 Ma; Henjes-Kunst and Kreuzer 2003). Although there is only limited Nd isotope data from the Admiralty Intrusives in north Victoria Land (Borg et al., 1986), they have a similar range of εNd values to those from the Ford Granodiorite suite (Fig. 15A). The ages of these rocks were constrained by Rb–Sr isochrons to the range 393–364 Ma and, thus, generally older than the Ford Granodiorite suite. However, Henjes-Kunst and

Kreuzer (2003) report Ar–Ar biotite ages and one U–Pb zircon age from other Admiralty Intrusive rocks in the range 371–354 Ma, which casts some doubt about the veracity of the Rb–Sr ages. Assuming contemporaneity between the Ford Granodiorite suite and the Admiralty Intrusives, the Nd isotope data suggest both were derived from an isotopically similar source.

In the Western Province of New Zealand, Devonian–Carboniferous igneous rocks coeval with the Ford Granodiorite suite include the Karamea–Paringa suite (371–351 Ma; Tulloch et al, 2009; Sagar and Palin, 2013) and the Ridge–Tobin suite (355–342 Ma; Tulloch et al, 2009). Granites from the volumetrically dominant Karamea suite have εNd values of -3 to -9 and estimated magma $\delta^{18}O$ values of 10.8 to 12.5‰ (Tulloch et al., 2009), which indicates that these granites were derived primarily from a metasedimentary source. Younger granite suites from the Western Province generally have more radiogenic εNd and $\varepsilon Hf_t$ zircon values (Fig. 15A, B) and more mantle-like $\delta^{18}O$ values than the Ford Granodiorite suite. In the Western Province, the high $\delta^{18}O$ values of the Karamea suite granites, their rapid emplacement (370–368 Ma; Tulloch et al., 2009), occurrence of contemporaneous mafic rocks (Turnbull et al., 2013), and partial melting at low pressures (~670°C at 0.5 GPa; Scott et al., 2011) may indicate a period of lithospheric extension and asthenospheric upwelling. Scott et al. (2011) suggest that crustal thinning may have been related to slab rollback or subduction cessation along this portion of the Gondwana margin. The lack of similar trends towards more radiogenic εNd values over time in Devonian–Carboniferous granites in western Marie Byrd Land and north Victoria Land (Fig. 15A) and the paucity of associated mafic rocks does not support a period of back-arc extension in these regions at this time. Therefore, the effects of slab rollback and lithospheric extension may be confined to the Western Province of New Zealand, which may have occupied a position closer to the subduction trench in the Devonian–Carboniferous (Veevers, 2012).

Overall, the changes in isotope composition and source characteristics recorded by arc-related granitoids from eastern Australia to north Victoria Land to the Western Province of New Zealand and Marie Byrd Land may relate to an along-arc change from the typical extensional accretionary mode in eastern Australia to a neutral or an advancing mode in West Antarctica, and to an across-arc difference in distance from the trench between the New Zealand fragments of Zealandia and western Marie Byrd Land.

## CONCLUSIONS

In the Ford Ranges of Marie Byrd Land, new U–Pb ages and Hf-isotope compositions of detrital zircons from the Swanson Formation and equivalent metasedimentary rocks combined with published data reveals three principal age populations. The largest population comprises Neoproterozoic–Cambrian zircons with evolved Hf isotope values consistent with derivation from reworked Mesoproterozoic crust. These zircons were likely sourced from a region of igneous and metamorphic rocks associated with the Ross–Delamerian Orogen that now lies beneath the East Antarctic ice sheet. A second population of Mesoproterozoic detrital zircons with juvenile Hf isotope values is consistent with derivation from crust, or sedimentary derivatives of crust, similar to the gneiss that crops out in the Haag Nunataks and a granite clast that originated from a Mesoproterozoic orogenic belt located beneath the Antarctic ice sheet. A third population of Paleoproterozoic zircons could have been sourced from Precambrian basement exposed in the central Transantarctic Mountains. Detrital zircon age distributions and Hf isotope measurements from the (meta-) sedimentary rocks document a major crust-forming event in the Mesoproterozoic during the transition from Nuna (Columbia) to Rodinia and extensive crustal reworking during Ross–Delamerian orogenesis.

U–Pb ages of the Ford Granodiorite suite and Devonian–Carboniferous granites and diatexites define a short-lived period of magmatism in the Ford Ranges from 375to 345 Ma. The Hf and O isotope compositions of zircons from the oldest Ford Granodiorite suite samples are consistent with mixing of a juvenile magma with Swanson Formation in an active arc setting. Isotope values of zircons from the younger members of the Ford Granodiorite suite are also compatible with this petrogenetic scenario but require a larger proportion of Swanson Formation. Alternatively, these younger members may have been derived by anatectic reworking of older members of the Ford Granodiorite suite and mixing with Swanson Formation either *en masse* or as melts in the deep crust. The Devonian–Carboniferous granites and diatexites from the Fosdick complex represent Ford Granodiorite suite magmas or anatectic melt derived from early-crystallized members of the suite that assimilated Swanson Formation *en masse* or mixed with anatectic melt derived from the Swanson Formation. The Ford Granodiorite suite and the granites and diatexites do not show the same temporal trends in source compositions recorded by similar-age circum-Pacific granite suites in Eastern Australia, north Victoria Land and the Western Province of New Zealand.

## ACKNOWLEDGEMENTS

This work was supported by the National Science Foundation under Grant No. ANT0944615 to MB at the University of Maryland, and Grant Nos OPP-0338279 and OPP-0944600 to CS at Colorado College. The authors acknowledge used of facilities in the NanoCenter and the NISP-Lab at the University of Maryland, which are supported as a MRSEC Shared Experimental Facility. CY was partially funded by a post-graduate scholarship from the National Science and Engineering Research Council of Canada. We thank T. Burton, K. Emery and D. Uhlmann for their contribution to field logistics and safety, and Kenn Borek Air and Raytheon Polar Services personnel for transportation and logistical support. We thank M. Pecha and N. Giesler for assistance with data collection at the Arizona LaserChron Center, which is supported by funding from NSF-EAR1032156, and Bin Fu for assistance with sample preparation and analytical work at the Australian National University. John Valley at the University of Wisconsin provided the whole-rock oxygen isotope results. Finally, we thank M.J. Flowerdew and R.J. Pankhurst for thorough and constructive reviews, and C. Miller for editorial comments and advice.

**REFERENCES**

Adams, C. J. 1986. Geochronological studies of the Swanson Formation of Marie Byrd Land, West Antarctica, and correlation with northern Victoria Land, East Antarctica and the South Island, New Zealand. New Zealand Journal of Geology and Geophysics, v. 29, p. 345–358. doi: 10.1080/00288306.1986.10422157.

Adams, C. J., 1987, Geochronology of granite terranes in the Ford Ranges, Marie Byrd Land, West Antarctica: New Zealand Journal of Geology and Geophysics, v. 30, p. 51–72. doi:10.1080/00288306.1987.10422193.

Adams, C. J., 2004, Rb-Sr age and strontium isotope characteristics of the Greenland Group, Buller Terrane, New Zealand, and correlations at the east Gondwanaland margin: New Zealand Journal of Geology and Geophysics, v. 47, p. 189–200. doi:10.1080/00288306.2004.9515047.

Adams, C. J., 2010, Lost Terranes of Zealandia: possible development of late Paleozoic and early Mesozoic sedimentary basins at the southwest Pacific margin of Gondwana: Andean Geology, v. 37, p. 442–454. doi:10.5027/andgeoV37n2-a10.

Adams, C. J., Pankhurst, R. J., Maas, R., and Millar, I. L., 2005, Nd and Sr isotopic signatures of metasedimentary rocks around the South Pacific margin and implications for their provenance: Geological Society, London, Special Publications, v. 246, no. 1, p. 113–141. doi: 10.1144/GSL.SP.2005.246.01.04.

Adams, C. J., Mortimer, N., Campbell, H. J., and Griffin, W. L., 2013, The mid-Cretaceous transition from basement to cover within sedimentary rocks in eastern New Zealand; evidence from detrital zircon age patterns: Geological Magazine, v. 150, p. 455–478. doi:10.1017/s0016756812000611.

Allibone, A., and Wysoczanski, R., 2002, Initiation of magmatism during the Cambrian-Ordovician Ross Orogeny in southern Victoria Land, Antarctica: Geological Society of America Bulletin, v. 114, p. 1007–1018. doi:10.1130/0016-7606(2002)114<1007:iomdtc>2.0.co;2.

Bolhar, R., Weaver, S. D., Whitehouse, M. J., Palin, J. M., Woodhead, J. D., and Cole, J. W., 2008, Sources and evolution of arc magmas inferred from coupled O and Hf isotope systematics of plutonic zircons from the Cretaceous Separation Point Suite (New

Zealand): Earth and Planetary Science Letters, v. 268, p. 312–324. doi:10.1016/j.epsl.2008.01.022.

Bomparola, R. M., Ghezzo, C., Belousova, E., Griffin, W. L., and O'Reilly, S. Y., 2007, Resetting of the U–Pb Zircon System in Cambro-Ordovician Intrusives of the Deep Freeze Range, Northern Victoria Land, Antarctica: Journal of Petrology, v. 48, p. 327–364. doi:10.1093/petrology/egl064.

Borg, S. G., and DePaolo, D. J., 1991, A tectonic model of the Antarctic Gondwana margin with implications for southeastern Australia: isotopic and geochemical evidence: Tectonophysics, v. 196, p. 339–358. doi:10.1016/0040-1951(91)90329-Q.

Borg, S., Stump, E., and Holloway, J., 1986, Granitoids of northern Victoria Land, Antarctica: A reconnaissance study of field relations, petrography, and geochemistry: Antarctic Research Series, v. 46, p. 115–188.

Borg, S. G., Stump, E., Chappell, B. W., McCulloch, M. T., Wyborn, D., Armstrong, R. L., and Holloway, J. R., 1987, Granitoids of northern Victoria Land, Antarctica; implications of chemical and isotopic variations to regional crustal structure and tectonics: American Journal of Science, v. 287, p. 127–169. doi:10.2475/ajs.287.2.127.

Bradshaw, J. D., Andrews, P. B., and Field, B. D., 1983, Swanson Formation and related rocks of Marie Byrd Land and a comparison with the Robertson Bay Group of northern Victoria Land *in* Oliver, R.K., James, P.R., and Jago, J.B. (Eds). Antarctic Earth Science. Cambridge University Press: Cambridge, United Kingdom, p. 274–279.

Bradshaw, J. D., Vaughan, A. P., Millar, I. L., Flowerdew, M. J., Trouw, R. A., Fanning, C., and Whitehouse, M. J., 2012, Permo-Carboniferous conglomerates in the Trinity Peninsula Group at View Point, Antarctic Peninsula: sedimentology, geochronology and isotope evidence for provenance and tectonic setting in Gondwana: Geological Magazine, v. 149, p. 626–644. doi:10.1017/S001675681100080X.

Brown, M., 1973. The Definition of Metatexis, Diatexis and Migmatite. Proceedings of the Geologists' Association, 84, 371–382. doi:10.1016/S0016-7878(73)80021-5

Cawood, P. A., 2005, Terra Australis Orogen: Rodinia breakup and development of the Pacific and Iapetus margins of Gondwana during the Neoproterozoic and Paleozoic: Earth-Science Reviews, v. 69, p. 249–279. doi:10.1016/j.earscirev.2004.09.001.

Cecil, M. R., Gehrels, G. E., Ducea, M. N., and Patchett, P. J., 2011, U-Pb-Hf characterization of the central Coast Mountains Batholith; implications for petrogenesis and crustal architecture: Lithosphere, v. 3, p. 247–260. doi:10.1130/l134.1.

Chappell, B. W., White, A. J. R., and Hine, R., 1988, Granite provinces and basement terranes in the Lachlan Fold Belt, southeastern Australia: Australian Journal of Earth Sciences, v. 35, p. 505–521. doi:10.1080/08120098808729466.

Clemens, J.D., and Stevens, G., 2012, What controls chemical variation in granitic magmas?: Lithos, v. 134–135, p. 317–329, doi:10.1016/j.lithos.2012.01.001.

Clemens, J.D., Stevens, G., and Farina, F., 2011, The enigmatic sources of I-type granites: The peritectic connexion: Lithos, v. 126, p. 174–181, doi:10.1016/j.lithos.2011.07.004.

Collins, W. J., 2002, Nature of extensional accretionary orogens: Tectonics, v. 21, p. 6-1–6-12. doi:10.1029/2000tc001272.

Collins, W. J., Belousova, E. A., Kemp, A. I. S., and Murphy, J. B., 2011, Two contrasting Phanerozoic orogenic systems revealed by hafnium isotope data: Nature Geosci, v. 4, p. 333–337. doi:10.1038/ngeo1127.

Dallai, L., Ghezzo, C., and Sharp, Z. D., 2003, Oxygen isotope evidence for crustal assimilation and magma mixing in the Granite Harbour Intrusives, northern Victoria Land, Antarctica: Lithos, v. 67, p. 135–151. doi:10.1016/S0024-4937(02)00267-0.

DePaolo, D. J., 1981, Trace element and isotopic effects of combined wallrock assimilation and fractional crystallization: Earth and Planetary Science Letters, v. 53, p. 189–202. doi:10.1016/0012-821X(81)90153-9.

DiVenere, V. J., Kent, D. V., and Dalziel, I. W. D., 1994, Mid-Cretaceous paleomagnetic results from Marie Byrd Land, West Antarctica; a test of post-100 Ma relative motion between East and West Antarctica: Journal of Geophysical Research, v. 99, p. 15115–15139. doi:10.1029/94jb00807.

DiVenere, V., Kent, D. V., and Dalziel, I. W. D., 1995, Early Cretaceous paleomagnetic results from Marie Byrd Land, West Antarctica: Implications for the Weddellia collage of crustal blocks: Journal of Geophysical Research: Solid Earth, v. 100, p. 8133–8151. doi:10.1029/95jb00042.

Di Vincenzo, G., Grande, A., and Rossetti, F., 2014, Paleozoic siliciclastic rocks from northern Victoria Land (Antarctica): Provenance, timing of deformation, and implications for the Antarctica-Australia connection: Geological Society of America Bulletin, doi:10.1130/b31034.1.

Dhuime, B., Hawkesworth, C., and Cawood, P., 2011, When Continents Formed: Science, v. 331, p. 154–155. doi:10.1126/science.1201245.

Elliot, D. H., Fanning, C. M., and Hulett, S. R. W., 2014, Age provinces in the Antarctic craton: Evidence from detrital zircons in Permian strata from the Beardmore Glacier region, Antarctica: Gondwana Research. doi: 10.1016/j.gr.2014.03.013.

Finn, C., Moore, D., Damaske, D., and Mackey, T., 1999, Aeromagnetic legacy of early Paleozoic subduction along the Pacific margin of Gondwana: Geology, v. 27, p. 1087-1090. doi:10.1130/0091-7613(1999)027<1087:aloeps>2.3.co;2.

Fioretti, A. M., Visona, D., Cavazzini, G., and Lombardo, B., 1997, Devonian magmatism; implications for the evolution of northern Victoria Land, Antarctica, and correlation with southeastern Australia and northeastern Tasmania: International Symposium on Antarctic Earth Sciences, v. 7, p. 293–296.

Flowerdew, M. J., Millar, I. L., Curtis, M. L., Vaughan, A. P. M., Horstwood, M. S. A., Whitehouse, M. J., and Fanning, C. M., 2007, Combined U-Pb geochronology and Hf isotope geochemistry of detrital zircons from early Paleozoic sedimentary rocks, Ellsworth-Whitmore Mountains Block, Antarctica: Geological Society of America Bulletin, v. 119, p. 275–288. doi:10.1130/b25891.1.

Flowerdew, M. J., Millar, I. L., and Vaughan, A. P. M., 2006a, Potential of Combined U-Pb Geochronology and Hf isotope Geochemical Studies on Zircon to Aid Sedimentary Provenance within Antarctica: Examples from West Antarctica: Terra Antarctica Reports, v. 12, p. 57–64.

Flowerdew, M., Millar, I., Vaughan, A., Horstwood, M., and Fanning, C., 2006b, The source of granitic gneisses and migmatites in the Antarctic Peninsula: a combined U–Pb SHRIMP and laser ablation Hf isotope study of complex zircons: Contributions to Mineralogy and Petrology, v. 151, no. 6, p. 751–768. doi: 10.1007/s00410-006-0091-6.

Foster, D. A., Gray, D. R., Spaggiari, C., Kamenov, G., and Bierlein, F. P., 2009, Palaeozoic Lachlan orogen, Australia; accretion and construction of continental crust in a marginal ocean setting: isotopic evidence from Cambrian metavolcanic rocks: Geological Society, London, Special Publications, v. 318, p. 329–349. doi:10.1144/sp318.12.

Gehrels, G. E., Valencia, V. A., and Ruiz, J., 2008, Enhanced precision, accuracy, efficiency, and spatial resolution of U-Pb ages by laser ablation–multicollector–inductively coupled plasma–mass spectrometry: Geochemistry, Geophysics, Geosystems, v. 9, p. Q03017. doi:10.1029/2007gc001805.

Glen, R. A., 2005, The Tasmanides of eastern Australia: Geological Society, London, Special Publications, v. 246, p. 23–96. doi:10.1144/gsl.sp.2005.246.01.02.

Glen, R. A., Saeed, A., Quinn, C. D., and Griffin, W. L., 2011, U–Pb and Hf isotope data from zircons in the Macquarie Arc, Lachlan Orogen: Implications for arc evolution and Ordovician palaeogeography along part of the east Gondwana margin: Gondwana Research, v. 19, p. 670–685. doi:10.1016/j.gr.2010.11.011.

Goodge, J., and Fanning, C., 2002, Precambrian crustal history of the Nimrod Group, central Transantarctic Mountains, in Proceedings Antarctica at the Close of a Millennium, Proceedings of the 8th International Symposium on Antarctic Earth Science. Royal Society of New Zealand Bulletin, Volume 35, p. 43–50.

Goodge, J. W., and Finn, C. A., 2010, Glimpses of East Antarctica: Aeromagnetic and satellite magnetic view from the central Transantarctic Mountains of East Antarctica: Journal of Geophysical Research: Solid Earth, v. 115, p. B09103. doi:10.1029/2009jb006890.

Goodge, J. W., Fanning, C. M., and Bennett, V. C., 2001, U–Pb evidence of ~1.7 Ga crustal tectonism during the Nimrod Orogeny in the Transantarctic Mountains, Antarctica: implications for Proterozoic plate reconstructions: Precambrian Research, v. 112, p. 261-288. doi:10.1016/S0301-9268(01)00193-0.

Goodge, J. W., Fanning, C. M., Devon, M. B., Licht, K. J., and Emerson, F. P., 2010, Continuation of the Laurentian Grenville Province across the Ross Sea Margin of East Antarctica: The Journal of Geology, v. 118, p. 601–619. doi:10.1086/656385.

Goodge, J. W., Fanning, C. M., Norman, M. D., and Bennett, V. C., 2012, Temporal, Isotopic and Spatial Relations of Early Paleozoic Gondwana-Margin Arc Magmatism, Central Transantarctic Mountains, Antarctica: Journal of Petrology, v. 53, p. 2027–2065. doi:10.1093/petrology/egs043.

Goodge, J. W., Fanning, C. M., Vervoort J.D., and Fisher, C.M. 2013. Archean, Paleoproterozoic and Mesoproterozoic crust of Cetntral East Anrarctica: New insights on subglacial geology strengthen Rodinia ties to Western Laurentia. In Geological Society of America Abstracts with Programs, v. 45, No. 7.

Griffin, W. L., Pearson, N. J., Belousova, E., Jackson, S E , van Achterbergh, E , O,Reilly, S Y., and Shee, S. R., 2000, The Hf isotope composition of cratonic mantle: LAM-MC-ICPMS analysis of zircon megacrysts in kimberlites: Geochimica et Cosmochimica Acta, v. 64, p. 133–147. doi:10.1016/S0016-7037(99)00343-9.

Handler, M. R., Wysoczanski, R. J., and Gamble, J. A., 2003, Proterozoic lithosphere in Marie Byrd Land, West Antarctica; Re-Os systematics of spinel peridotite xenoliths: Chemical geology, v. 196, p. 131–145. doi:10.1016/s0009-2541(02)00410-2.

Harley, S. L., Fitzsimons, I. C. W., and Zhao, Y., 2013, Antarctica and supercontinent evolution: historical perspectives, recent advances and unresolved issues: Geological Society, London, Special Publications, v. 383, p. 1–34. doi:10.1144/SP383.9.

Hawkesworth, C. J., and Kemp, A. I. S., 2006, Using hafnium and oxygen isotopes in zircons to unravel the record of crustal evolution: Chemical geology, v. 226, p. 144–162. doi:10.1016/j.chemgeo.2005.09.018.

Henjes-Kunst, F., and Kreuzer, H., 2003, Mid-Paleozoic igneous activity in northern Victoria Land, Antarctica: implications of new geochronological data: Geologisches Jahrbuch B, v. 85, p. 271–302.

Hiess, J., Yi, K., Woodhead, J., Ireland, T., and Rattenbury, M., 2014, Gondwana margin evolution from zircon REE, O and Hf signatures of Western Province gneisses, Zealandia: Geological Society, London, Special Publications, v. 389, doi:10.1144/sp389.10.

Ireland, T. R., Floettmann, T., Fanning, C. M., Gibson, G. M., and Preiss, W. V., 1998, Development of the early Paleozoic Pacific margin of Gondwana from detrital-zircon ages across the Delamerian Orogen: Geology, v. 26, p. 243–246. doi:10.1130/0091-7613(1998)026<0243:dotepp>2.3.co;2.

Kemp, A. I. S., Hawkesworth, C. J., Collins, W. J., Gray, C. M., and Blevin, P. L., 2009, Isotopic evidence for rapid continental growth in an extensional accretionary orogen: The Tasmanides, eastern Australia: Earth and Planetary Science Letters, v. 284, p. 455–466. doi:10.1016/j.epsl.2009.05.011.

Kemp, A. I. S., Hawkesworth, C. J., Foster, G. L., Paterson, B. A., Woodhead, J. D., Hergt, J. M., Gray, C. M., and Whitehouse, M. J., 2007, Magmatic and Crustal Differentiation History of Granitic Rocks from Hf-O Isotopes in Zircon: Science, v. 315, p. 980–983. doi:10.1126/science.1136154.

Korhonen, F. J., Saito, S., Brown, M., Siddoway, C. S., and Day, J. M. D., 2010a, Multiple generations of granite in the Fosdick Mountains, Marie Byrd Land, West Antarctica; implications for polyphase intracrustal differentiation in a continental margin setting: Journal of Petrology, v. 51, p. 627–670. doi:10.1093/petrology/egp093.

Korhonen, F. J., Saito, S., Brown, M., and Siddoway, C. S., 2010b, Modeling multiple melt loss events in the evolution of an active continental margin: Lithos, v. 116, p. 230–248. doi:10.1016/j.lithos.2009.09.004.

Korhonen, F. J., Brown, M., Grove, M., Siddoway, C. S., Baxter, E. F., and Inglis, J. D., 2012, Separating metamorphic events in the Fosdick migmatite-granite complex, West Antarctica: Journal of Metamorphic Geology, v. 30, p. 165–192. doi:10.1111/j.1525-1314.2011.00961.x.

Kruskal, W. H., and Wallis, W. A., 1952, Use of Ranks in One-Criterion Variance Analysis: Journal of the American Statistical Association, v. 47, p. 583–621. doi:10.1080/01621459.1952.10483441.

Luyendyk, B. P., 1995, Hypothesis for Cretaceous rifting of East Gondwana caused by subducted slab capture: Geology, v. 23, p. 373–376. doi:10.1130/0091-7613(1995)023<0373:hfcroe>2.3.co;2.

Luyendyk, B.P., Cisowski, S., Smith, C.H., Richard, S. M., and Kimbrough, D.L., 1996, Paleomagnetic study of the northern Ford Ranges, western Marie Byrd Land, West Antarctica: a middle Cretaceous pole, and motion between West and East Antarctica? Tectonics, v. 15, p. 122–141. doi: 10.1029/95TC02524

McDonough, W. F., and Sun, S. s., 1995, The composition of the Earth: Chemical geology, v. 120, p. 223-253. doi:10.1016/0009-2541(94)00140-4.

McFadden, R. R., Siddoway, C. S., Teyssier, C., and Fanning, C. M., 2010, Cretaceous oblique extensional deformation and magma accumulation in the Fosdick Mountains migmatite-cored gneiss dome, West Antarctica: Tectonics, v. 29, TC4022. doi:10.1029/2009tc002492.

Miles, A., Graham, C., Hawkesworth, C., Gillespie, M., Dhuime, B., and Hinton, R., 2014, Using Zircon Isotope Compositions to Constrain Crustal Structure and Pluton Evolution: the Iapetus Suture Zone Granites in Northern Britain: Journal of Petrology, v. 55, p. 181–207. doi:10.1093/petrology/egt065.

Millar, I. L., and Pankhurst, R. J., 1987, Rb-Sr geochronology of the region between the Antarctic Peninsula and the Transantarctic Mountains; Haag Nunataks and Mesozoic granitoids: Geophysical Monograph, v. 40, p. 151–160. doi:10.1029/GM040p0151.

Mortimer, N., Hoernle, K., Hauff, F., Palin, J. M., Dunlap, W. J., Werner, R., and Faure, K., 2006, New constraints on the age and evolution of the Wishbone Ridge, Southwest Pacific Cretaceous microplates, and Zealandia-West Antarctica breakup: Geology, v. 34, p. 185–188. doi:10.1130/g22168.1.

Muir, R. J., Ireland, T. R., Weaver, S. D., and Bradshaw, J. D., 1994, Ion microprobe U-Pb zircon geochronology of granitic magmatism in the Western Province of the South Island, New Zealand: Chemical geology, v. 113, p. 171–189. doi:10.1016/0009-2541(94)90011-6.

Muir, R. J., Ireland, T. R., Weaver, S. D., and Bradshaw, J. D., 1996, Ion microprobe dating of Paleozoic granitoids; Devonian magmatism in New Zealand and correlations with Australia and Antarctica: Chemical geology, v. 127, p. 191–210. doi:10.1016/0009-2541(95)00092-5.

Mukasa, S. B., and Dalziel, I. W. D., 2000, Marie Byrd Land, West Antarctica; evolution of Gondwana's Pacific margin constrained by zircon U-Pb geochronology and feldspar common-Pb isotopic compositions: Geological Society of America Bulletin, v. 112, p. 611–627. doi:10.1130/0016-7606(2000)112<0611:mblwae>2.3.co;2.

Nebel-Jacobsen, Y., Münker, C., Nebel, O., and Mezger, K., 2011, Precambrian sources of Early Paleozoic SE Gondwana sediments as deduced from combined Lu–Hf and U–Pb systematics of detrital zircons, Takaka and Buller terrane, South Island, New Zealand: Gondwana Research, v. 20, p. 427–442. doi:http://dx.doi.org/10.1016/j.gr.2010.11.014.

O'Neil, J. R., and Chappell, B. W., 1977, Oxygen and hydrogen isotope relations in the Berridale batholith: Journal of the Geological Society, v. 133, p. 559–571. doi:10.1144/gsjgs.133.6.0559.

Pankhurst, R. J., Millar, I. L., Grunow, A. M., and Storey, B. C., 1993, The pre-Cenozoic magmatic history of the Thurston Island crustal block, West Antarctica: Journal of Geophysical Research, v. 98, p. 11835–11849. doi:10.1029/93jb01157.

Pankhurst, R. J., Weaver, S. D., Bradshaw, J. D., Storey, B. C., and Ireland, T. R., 1998, Geochronology and geochemistry of pre-Jurassic superterranes in Marie Byrd Land, Antarctica: Journal of Geophysical Research, v. 103, p. 2529–2547. doi:10.1029/97jb02605.

Patiño Douce, A. E., and Harris, N., 1998, Experimental Constraints on Himalayan Anatexis: Journal of Petrology, v. 39, p. 689–710. doi:10.1093/petroj/39.4.689.

Paulsen, T. S., Encarnación, J., Grunow, A. M., Valencia, V. A., Pecha, M., Layer, P. W., and Rasoazanamparany, C , 013, Age and significance of ’outboard’ high-grade metamorphics and intrusives of the Ross orogen, Antarctica: Gondwana Research, v. 24, p. 349–358. doi:10.1016/j.gr.2012.10.004.

Paulsen, T. S., Encarnación, J., Grunow, A. M., Valencia, V. A., Layer, P. W., Pecha, M., Stump, E., Roeske, S., Thao, S., and Rasoazanamparany, C., 2015, Detrital mineral ages from the Ross Supergroup, Antarctica: Implications for the Queen Maud terrane and outboard sediment provenance on the Gondwana margin: Gondwana Research, v. 27, no. 1, p. 377–391, doi:10.1016/j.gr.2013.10.006.

Richard, S. M., Smith, C. H., Kimbrough, D. L., Fitzgerald, P. G., Luyendyk, B. P., and McWilliams, M. O., 1994, Cooling history of the northern Ford Ranges, Marie Byrd Land, West Antarctica: Tectonics, v. 13, p. 837–857. doi:10.1029/93tc03322.

Rowell, A. J., Rees, M. N., Dubendorfer, E. M., Wallin, E. T., Van Schmus, W. R., and Smith, E. I., 1993, An active Neoproterozoic margin: evidence from the Skelton Glacier area, Transantarctic Mountains: Journal of the Geological Society, v. 150, p. 677–682. doi:10.1144/gsjgs.150.4.0677.

Sagar, M. W., and Palin, J. M., 2013, Carboniferous U–Pb zircon age for S-type Karamea Suite Redjacket Granite, Paparoa Metamorphic Core Complex lower plate, northern Westland: New Zealand Journal of Geology and Geophysics, v. 56, p. 109–120. doi:10.1080/00288306.2013.788525.

Scott, J. M., Cooper, A. F., Palin, J. M., Tulloch, A. J., Kula, J., Jongens, R., Spell, T. L., and Pearson, N. J., 2009, Tracking the influence of a continental margin on growth of a magmatic arc, Fiordland, New Zealand, using thermobarometry, thermochronology, and zircon U-Pb and Hf isotopes: Tectonics, v. 28, p. TC6007. doi:10.1029/2009tc002489.

Scott, J., Muhling, J. R., Fletcher, I., Billia, M., Palin, J. M., Elliot, T., and Guenter, C., 2011, The relationship of Palaeozoic metamorphism and S-type magmatism on the paleo-Pacific Gondwana margin: Lithos, v. 127, p. 522–534. doi:10.1016/j.lithos.2011.09.008.

Skjerlie, K. P., and Johnston, A. D., 1993, Fluid-Absent Melting Behavior of an F-Rich Tonalitic Gneiss at Mid-Crustal Pressures: Implications for the Generation of Anorogenic Granites: Journal of Petrology, v. 34, p. 785–815. doi:10.1093/petrology/34.4.785.

Siddoway, C. S., Baldwin, S. L., Fitzgerald, P. G., Fanning, C. M., and Luyendyk, B. P., 2004a, Ross Sea mylonites and the timing of intracontinental extension within the West Antarctic rift system: Geology, v. 32, p. 57–60. doi:10.1130/g20005.1.

Siddoway, C. S., Richard, S. M., Fanning, C. M., and Luyendyk, B. P., 2004b, Origin and emplacement of a Middle Cretaceous gneiss dome, Fosdick Mountains, West Antarctica: Special Paper - Geological Society of America, v. 380, p. 267–294. doi: 10.1130/0-8137-2380-9.267.

Siddoway, C. S., and Fanning, C. M., 2009, Paleozoic tectonism on the East Gondwana margin: Evidence from SHRIMP U–Pb zircon geochronology of a migmatite‚Äìgranite complex in West Antarctica: Tectonophysics, v. 477, p. 262–277. doi: 10.1016/j.tecto.2009.04.021.

Smith, C. H., 1996, Migmatites of the Alexandra Mountains, West Antarctica: Pressure-Temperature conditions of formation and regional context: Geologisches Jahrbuch, v. B52, p. 169–178.

Solar, G.S., and Brown, M., 2001a, Petrogenesis of migmatites in Maine, USA: Possible source of peraluminous leucogranite in plutons: Journal of Petrology, v. 42, p. 789–823, doi:10.1093/petrology/42.4.789.

Storey, B. C., Leat, P. T., Weaver, S. D., Pankhurst, R. J., Bradshaw, J. D., and Kelley, S., 1999, Mantle plumes and Antarctica-New Zealand rifting; evidence from Mid-Cretaceous mafic dykes: Journal of the Geological Society of London, v. 156, p. 659–671. doi:10.1144/gsjgs.156.4.0659.

Storey, B. C., Pankhurst, R. J., and Johnson, A. C., 1994, The Grenville Province within Antarctica; a test of the SWEAT hypothesis: Journal of the Geological Society of London, v. 151, p. 1–4. doi:10.1144/gsjgs.151.1.0001.

Tera, F., and Wasserburg, G. J., 1972, U-Th-Pb systematics in three Apollo 14 basalts and the problem of initial Pb in lunar rocks: Earth and Planetary Science Letters, v. 14, p. 281–304. doi:10.1016/0012-821X(72)90128-8.

Tochilin, C. J., Reiners, P. W., Thomson, S. N., Gehrels, G. E., Hemming, S. R., and Pierce, E. L., 2012, Erosional history of the Prydz Bay sector of East Antarctica from detrital apatite and zircon geo- and thermochronology multidating: Geochemistry, Geophysics, Geosystems, v. 13, p. Q11015. doi:10.1029/2012gc004364.

Tukey, J. W., 1977, Exploratory Data Analysis: Addison-Wesley, 688 pp.

Tulloch, A. J., Ramezani, J., Kimbrough, D. L., Faure, K., and Allibone, A. H., 2009, U-Pb geochronology of mid-Paleozoic plutonism in western New Zealand; implications for S-type granite generation and growth of the east Gondwana margin: Geological Society of America Bulletin, v. 121, p. 1236–1261. doi:10.1130/b26272.1.

Turnbull, R. E., Tulloch, A. J., and Ramezani, J., 2013, Zetland Diorite, Karamea Batholith, west Nelson; field relationships, geochemistry and geochronology demonstrate links to the Carboniferous Tobin Suite: New Zealand Journal of Geology and Geophysics, v. 56, p. 83–99. doi:10.1080/00288306.2013.775166.

Valley, J. W., Chiarenzelli, J. R., and McLelland, J. M., 1994, Oxygen isotope geochemistry of zircon: Earth and Planetary Science Letters, v. 126, p. 187–206. doi:10.1016/0012-821X(94)90106-6.

Valley, J. W., Kitchen, N., Kohn, M. J., Niendorf, C. R., and Spicuzza, M. J., 1995, UWG-2, a garnet standard for oxygen isotope ratios; strategies for high precision and accuracy with laser heating: Geochimica et Cosmochimica Acta, v. 59, p. 5223–5231. doi: 10.1016/0016-7037(95)00386-X

Valley, J. W., Kinny, P. D., Schulze, D. J., and Spicuzza, M. J., 1998, Zircon megacrysts from kimberlite: oxygen isotope variability among mantle melts: Contributions to Mineralogy and Petrology, v. 133, p. 1–11. doi:10.1007/s004100050432.

Valley, J. W., Bindeman, I. N., and Peck, W. H., 2003, Empirical calibration of oxygen isotope fractionation in zircon: Geochimica et Cosmochimica Acta, v. 67, p. 3257–3266. doi:10.1016/s0016-7037(03)00090-5.

Veevers, J. J., 2012, Reconstructions before rifting and drifting reveal the geological connections between Antarctica and its conjugates in Gondwanaland: Earth-Science Reviews, v. 111, p. 249–318. doi:10.1016/j.earscirev.2011.11.009.

Vervoort, J. D., and Jonathan Patchett, P., 1996, Behavior of hafnium and neodymium isotopes in the crust: Constraints from Precambrian crustally derived granites: Geochimica et Cosmochimica Acta, v. 60, p. 3717–3733. doi:10.1016/0016-7037(96)00201-3.

Vervoort, J. D., and Blichert-Toft, J., 1999, Evolution of the depleted mantle: Hf isotope evidence from juvenile rocks through time: Geochimica et Cosmochimica Acta, v. 63, p. 533–556. doi:10.1016/S0016-7037(98)00274-9.

Vervoort, J. D., Patchett, P. J., Blichert-Toft, J., and Albarède, F., 1999, Relationships between Lu–Hf and Sm–Nd isotopic systems in the global sedimentary system: Earth and Planetary Science Letters, v. 168, p. 79–99. doi:10.1016/S0012-821X(99)00047-3.

Vetter, U., and Tessensohn, F., 1987, S- and I-Type granitoids of North Victoria Land, Antarctica, and their inferred geotectonic setting: Geologische Rundschau, v. 76, p. 233–243. doi:10.1007/BF01820585.

Wandres, A.M. and Bradshaw, J.D. 2005. New Zealand tectonostratigraphy and implications from conglomeratic rocks for the configuration of the SW Pacific of Gondwana. In: Vaughan, A.P.M., Leat, P.T., and Pankhurst, R (Eds), Terrane Processes at the Margin of Gondwana. Geological Society, London, Special Publication v. 246, p. 179–206. doi: 10.1144/GSL.SP.2005.246.01.06.

Weaver, S. D., Adams, C. J., Pankhurst, R. J., and Gibson, I. L., 1992, Granites of Edward VII Peninsula, Marie Byrd Land; anorogenic magmatism related to Antarctic-New Zealand rifting: Special Paper - Geological Society of America, v. 272, p. 281–290. doi:10.1130/SPE272-p281.

Weaver, S. D., Bradshaw, J. D., and Adams, C. J., 1991, Granitoids of the Ford Ranges, Marie Byrd Land, Antarctica, Geological Evolution of Antarctica, Volume 5: International, Cambridge University Press : Cambridge - New York, International, p. 345–351.

Weaver, S. D., Storey, B. C., Pankhurst, R. J., Mukasa, S. B., DiVenere, V. J., and Bradshaw, J. D., 1994, Antarctica-New Zealand rifting and Marie Byrd Land lithospheric magmatism linked to ridge subduction and mantle plume activity: Geology, v. 22, p. 811–814. doi:10.1130/0091-7613(1994)022<0811:anzram>2.3.co;2.

Yakymchuk, C., Siddoway, C. S., Fanning, C. M., McFadden, R., Korhonen, F. J., and Brown, M., 2013a, Anatectic reworking and differentiation of continental crust along the active margin of Gondwana; a zircon Hf-O perspective from West Antarctica: Special Publication - Geological Society of London v. 383. doi:10.1144/sp383.7.

Yakymchuk, C., Brown, M., Ivanic, T. J., and Korhonen, F. J., 2013b, Leucosome distribution in migmatitic paragneisses and orthogneisses: A record of self-organized melt migration and entrapment in a heterogeneous partially-molten crust: Tectonophysics, v. 603, p. 136–154. doi:10.1016/j.tecto.2013.05.022.

Yakymchuk, C., Brown, M., Clark, C., Korhonen, F. J., Piccoli, P. M., Siddoway, C. S., Taylor, R. J. M., and Vervoort, J. D., 2015, Decoding polyphase migmatites using geochronology and phase equilibria modelling: Journal of Metamorphic Geology. doi: 10.1111/jmg.12117.

## FIGURE CAPTIONS

**Figure 1**. (**A**) Geometrical reconstruction of the East Gondwana active convergent margin (modified from Veevers, 2012, Fig. 4). (**B**) Map of part of Antarctica to show locations referred to in the text.

**Figure 2**. The inset at the top, left shows the location of the study area in western Marie Byrd Land in West Antarctica. The main map shows sample localities in the study area. The thick dashed line separating the Ross Province from the Amundsen Province is taken from Pankhurst et al. (1998). The inset at the bottom, right shows sample localities in the Fosdick migmatite–granite complex.

**Figure 3.** Histograms and normalized probability distribution curves of U–Pb ages retrieved from detrital zircon in the Swanson Formation (**A–C**) and metasedimentary rocks (**D–F**) outcropping in western Marie Byrd Land. All data from Table DR6 are plotted. (**G**) inherited grains (> 400 Ma) in the Ford Granodiorite suite, Devonian–Carboniferous granites, and diatexites (data from Pankhurst et al., 1998; Siddoway and Fanning, 2009; Korhonen et al., 2010b; Yakymchuk et al., 2013a; this study).

**Figure 4.** Cathodoluminescence images of representative zircon grains from the Swanson Formation and the Ford Granodiorite suite as well as Devonian–Carboniferous diatexites and granites from the Fosdick migmatite–granite complex. Ellipses mark the location of U–Pb, O and Hf isotope spot analyses. Cathodoluminescence images were collected on different dates and so exhibit some variation in quality/sharpness. The contrast of images of individual zircons was adjusted to best display internal zoning.

**Figure 5.** U–Pb Tera–Wasserberg (1972) concordia and probability density plots of zircon data from the Ford Granodiorite suite and Devonian–Carboniferous diatexites and granites from the Fosdick migmatite–granite complex. Data-point error ellipses are at 95% confidence. Age

uncertainties are reported at $\sigma$ confidence

**Figure 6.** Major and trace element data for samples as determined by XRF. Ford Granodiorite suite samples include data from Korhonen et al. (2010a), Weaver et al. (1992), Pankhurst et al. (1998) and Tulloch et al. (2009) as well as the new data from this study. FeO* represents total iron as ferrous. Trace elements are plotted as parts per million (ppm).

**Figure 7.** Chondrite-normalized (McDonough and Sun, 1995) rare earth element patterns of newly-analyzed samples from this study as well as additional data from Korhonen et al. (2010a) and Tulloch et al. (2009).

**Figure 8**. Sr–Nd isotopic compositions at 360 Ma of samples from this study and additional data from Korhonen et al. (2010a), Weaver et al. (1992), and Pankhurst et al. (1998). The two grey lines connect samples that represent exemplar isotopic end members of the Swanson Formation and the Ford Granodiorite suite, respectively, chosen so that the resulting mixing curves enclose the range of isotopic compositions for the granites and the diatexite. Tick marks along mixing curve are at 10% increments.

**Figure 9.** (**A**) Hf evolution diagram for detrital zircons from the Swanson Formation. Reference evolution line for depleted mantle (DM) is from Vervoort and Blichert-Toft (1999) and for new crust is from Dhuime et al. (2011). (**B**) Hf and O isotope values of detrital zircon from a sample of calc-silicate gneiss (8D27-10). The $\delta^{18}O$ value of the mantle ($5.3 \pm 0.6‰$) is from Valley et al. (1998). Newly crystallized zircons derived from partial melting of metasedimentary rocks are

expected to have $\delta^{18}$O values of ~8.5–12‰.

**Figure 10.** Plots of $\delta^{18}$Oand $\varepsilon Hf_t$ versus $^{238}U/^{206}Pb$ crystallization age for zircons from four Ford Granodiorite suite samples and two diatexites  Uncertainties are ± σ  for $\delta^{18}$O and $\varepsilon Hf_t$. The $\varepsilon Hf_t$ for new crust is taken from Dhuime et al. (2011; +12.2 ± 1.1) and $\delta^{18}$O for the mantle is from Valley et al. (1998; 5.3 ± 0.6‰). The $\varepsilon Hf_t$ (median value of -11.7 and an interquartile range of -3.5 to -19.9) and $\delta^{18}$O (8.5–12‰, with a mean value of 10.5‰) values chosen for the Swanson Formation are discussed in the text.

**Figure 11.** Hf evolution diagram to show data for detrital zircons from the Swanson Formation, igneous zircon from the Ford Granodiorite suite, zircon from the gneiss at Haag Nunataks (from Flowerdew et al., 2007), and zircon from granite clasts (from Goodge et al., 2013). Reference evolution lines for the depleted mantle (DM) are from Vervoort and Blichert-Toft (1999) and for new crust are from Dhuime et al. (2011). The dark grey εHf evolution lines from the gneiss at Haag Nunatak and ca. 1.2 Ga granite clast were constructed using the average $^{176}Lu/^{177}Hf$ value of crustal rocks (0.0115) and the light grey fields extend to ±1σ of this average (Vervoort and Patchett, 1996; Vervoort et al., 1999).

**Figure 12.** Box-and-whisker plots for $\varepsilon Hf_t$ and $\delta^{18}$Oversus $^{238}U/^{206}Pb$ zircon crystallization age for members of the Ford Granodiorite suite (dark grey boxes), and samples of the associated granites (open boxes) and diatexites (light gray boxes). The box represents the interquartile range (the middle 50% of the data from the 25$^{th}$ to the 75$^{th}$ percentile), the whiskers extend to 1.5 times the interquartile range and the crosses represent outliers. Data for samples MB.214, MB.219,

M5-G175 and C5-Is51a are from Pankhurst et al. (1998) and Yakymchuk et al. (2013a). The crystallization age for sample Y1-IG071 is taken to be 360 Ma, as discussed in the text. The $\varepsilon Hf_t$ for new crust is taken from Dhuime et al. (2011; +12.2 ± 1.1) and $\delta^{18}O$ for the mantle is from Valley et al. (1998; 5.3 ± 0.6‰). The $\varepsilon Hf_t$ (median value of -11.7 and an interquartile range of -3.5 to -19.9) and $\delta^{18}O$ (8.5–12‰, with a mean value of 10.5‰) values chosen for the Swanson Formation are discussed in the text.

**Figure. 13. (A)** Plots of $\delta^{18}$Oversus $\varepsilon Hf_t$ for individual zircons from the four newly-analyzed members of the Ford Granodiorite suite. Binary mixing lines connect representative end-members of each of the sources modeled—the mantle (Juv) and the Swanson Formation (SF). Small filled circles on each line display 10% increments. **(B)** Field to show the range of $\delta^{18}$Oand $\varepsilon Hf_t$ values for the data shown in (A). Binary mixing lines between anatectic melt derived from the Ford Granodiorite suite (FGD) and Swanson Formation either assimilated *en masse* or as anatectic melt separated from the Swanson Formation. Two representative end-member $\varepsilon Hf_t$ and $\delta^{18}O$ values are used to evaluate the contribution from the oldest and most juvenile end-members of the Ford Granodiorite suite. **(C)** Plots of $\delta^{18}O$ and $\varepsilon Hf_t$ values from individual zircons from granites and diatexites in the Fosdick migmatite–granite complex. The field for the full range of $\delta^{18}O$ and $\varepsilon Hf_t$ values retrieved from the Ford Granodiorite suite represents one of the end-member source compositions used in the modeling. Multiple binary mixing scenarios for the petrogenesis of the granites and diatexites are evaluated. Also shown in all three figures are end-member $\varepsilon Hf$ values for the mantle, corresponding to CHUR and a value expected for new crust, respectively. The $\delta^{18}O$ value of the mantle is 5 3 ± 0 6‰ (Valley et al., 1998). The $\varepsilon Hf_t$ (median value of -11.7 and an interquartile range of -3.5 to -19.9) and $\delta^{18}O$ (8.5–12‰, with a mean value of 10.5‰) values chosen for the Swanson Formation.

**Figure 14.** Ternary (Na+Ca)–(Fe*+Mg+Ti)–K plot (cf. Solar and Brown, 2001) of the full suite of granites and diatexites to assess different petrogenetic models. Starting materials and experimental melt compositions are taken from Skjerlie et al. (1993) and Patiño Douce and Harris (1998). The experimental melts from Skjerlie et al. (1993) were used as proxies for melts derived from the Ford Granodiorite suite while the experimental results of Patiño Douce and Harris (1998) were used to infer melt compositions derived from the Swanson Formation. The shaded areas represent the range of possible granite and diatexite compositions that may be achieved by assimilation or mixing between Ford Granodiorite suite compositions and Swanson Formation *en masse* or as anatectic melt separated from residue.

**Figure 15.** Compilation of whole rock Nd (**A**) and zircon Hf (**B**) isotope data for igneous rocks from the eastern Gondwana margin. Data sources include: the Ford Ranges of western Marie Byrd Land (Pankhurst et al., 1998; Korhonen et al., 2010; Yakymchuk et al., 2013a; this study), the Western Province of New Zealand (Muir et al., 1996; Scott et al., 2009; Tulloch et al., 2009), north Victoria Land (Borg et al., 1986; Armienti et al., 1990; Borg and DePaolo, 1991; Bomparola et al., 2007), and the Tasmanides (Kemp et al., 2007; Kemp et al., 2009 and references therein). Reference evolution lines for the depleted mantle (DM) are from Vervoort and Blichert-Toft (1999) for Hf and DePaolo (1981) for Nd. Hf isotope values for new crust are from Dhuime et al. (2011).

Figure 1
Click here to download Figure: fig1.eps

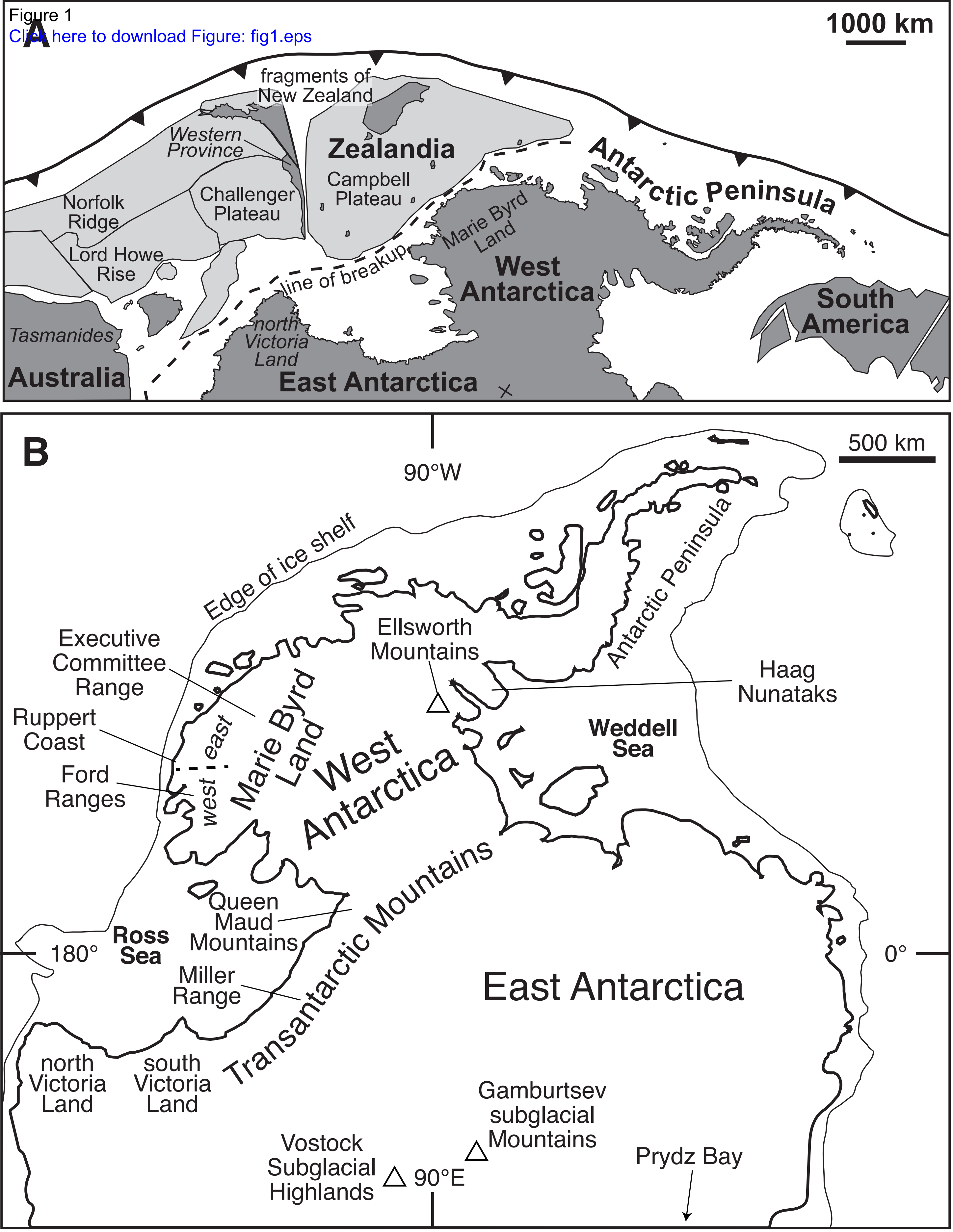


Figure 1
Yakymchuk et al.

Figure 2

Click here to download Figure: fig2.eps

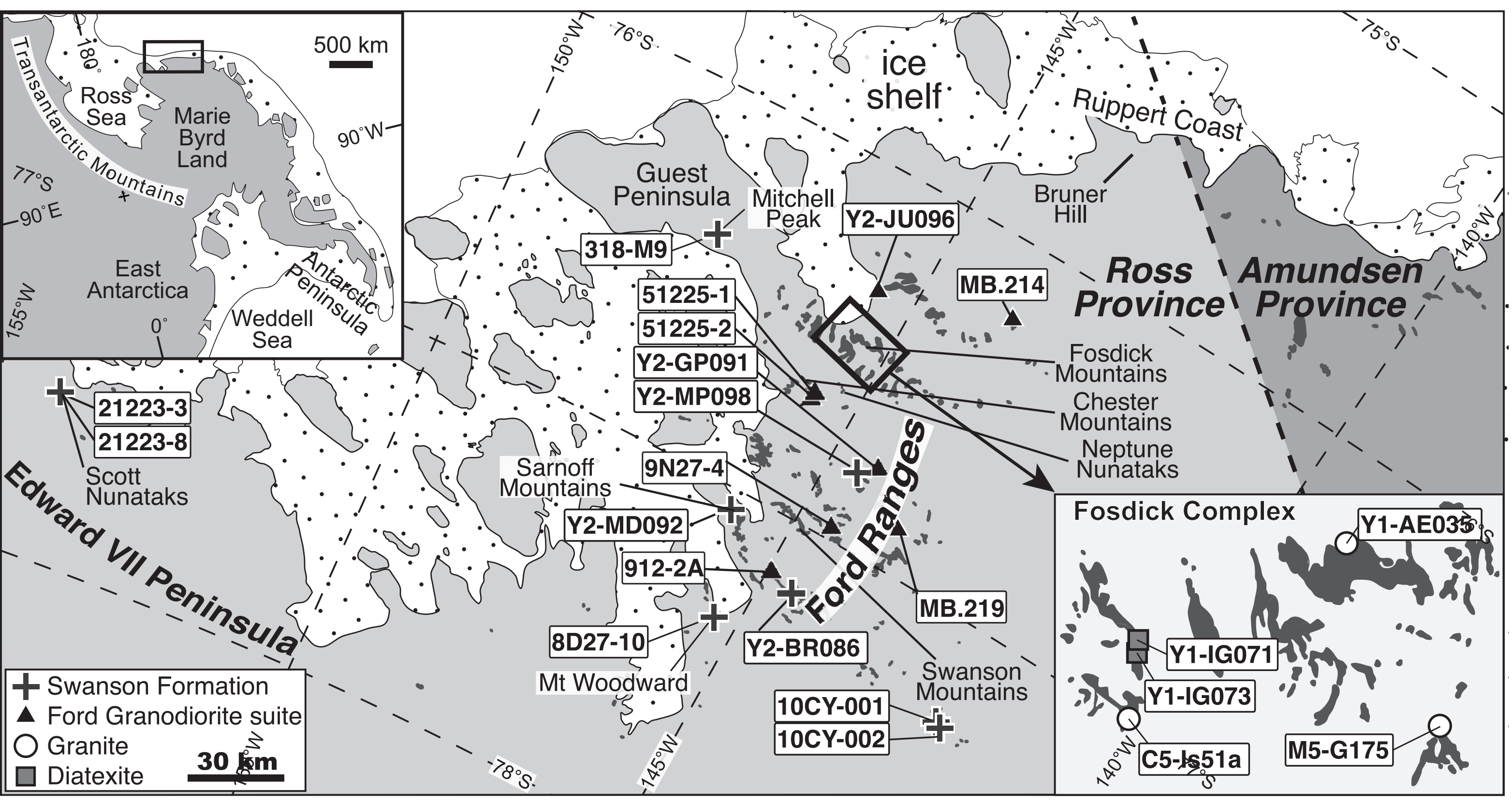


Yakymchuk et al.

Figure 2

Figure 3

Click here to download Figure: fig3.eps

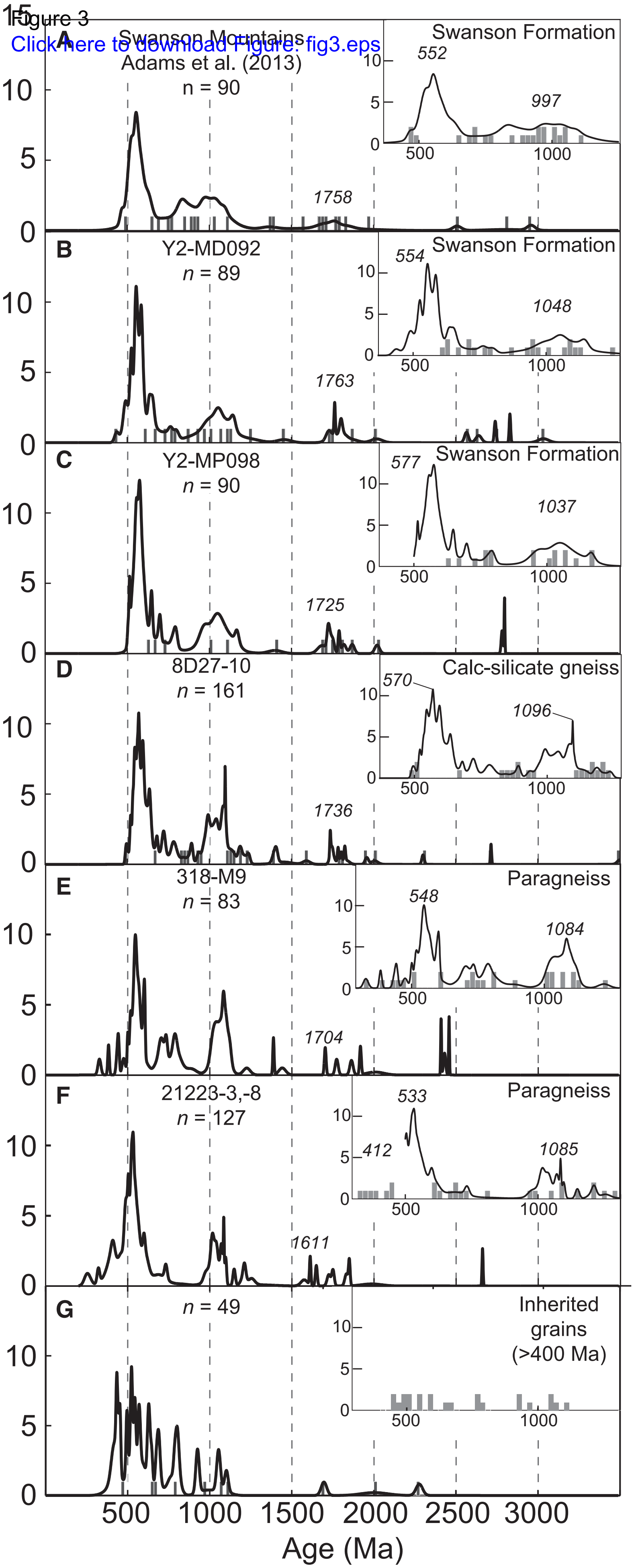


Figure 3
Yakymchuk et al.

Figure 4
Click here to download high resolution image

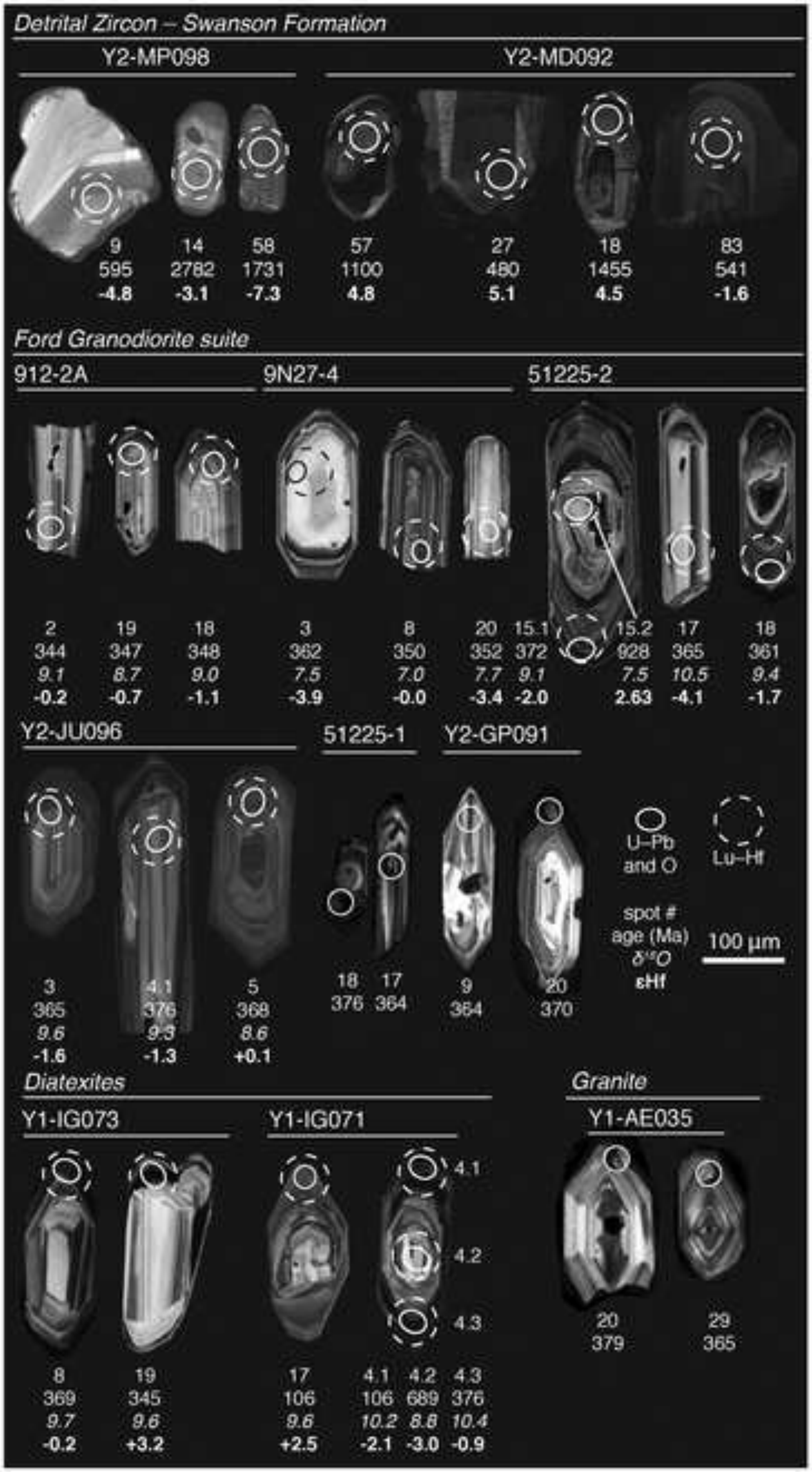


Figure 4
Yakymchuk et al.

Figure 5
Click here to download Figure: fig5.eps

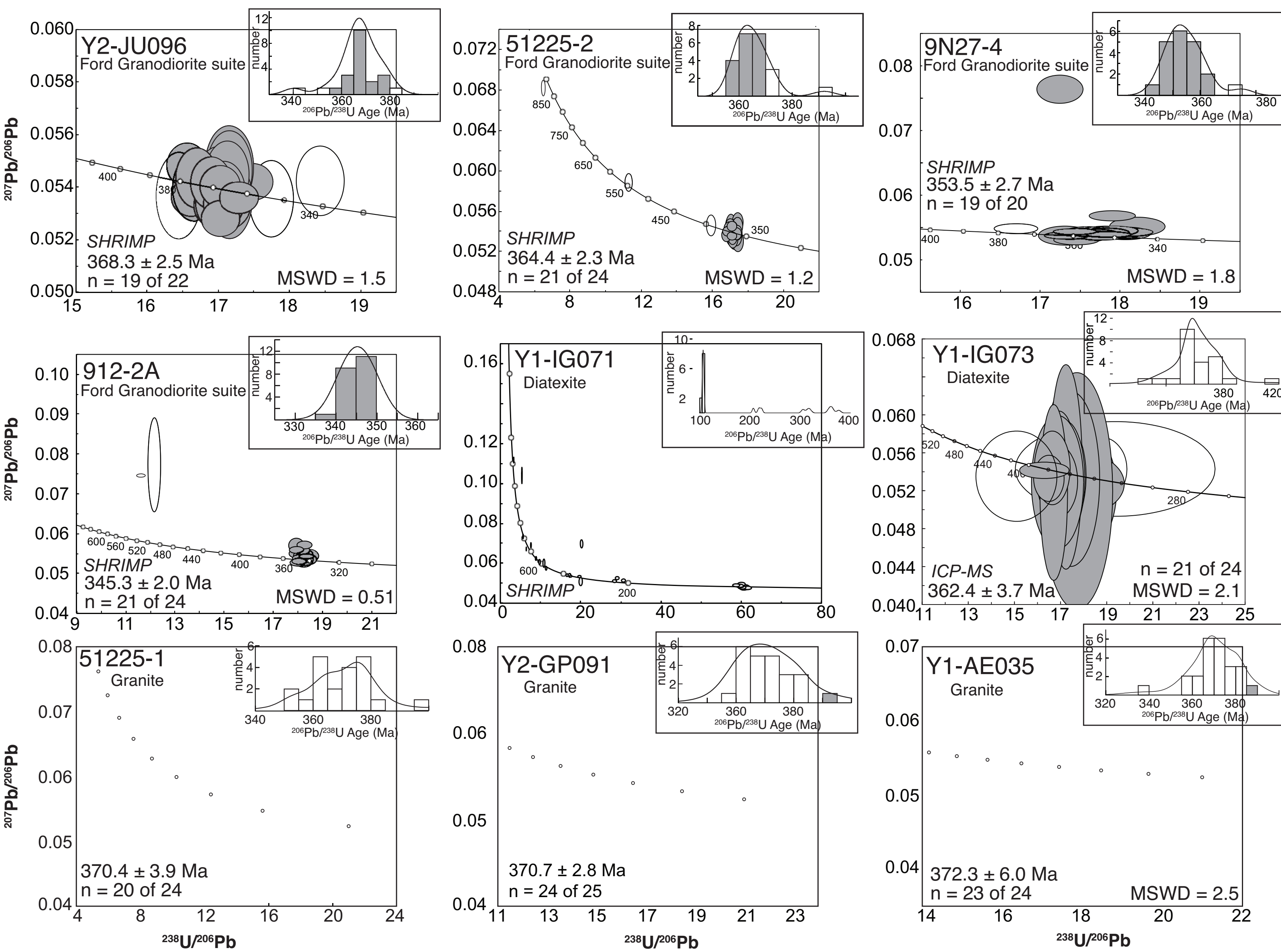


Figure 5
Yakymchuk et al.

Figure 6
Click here to download Figure: fig6.eps

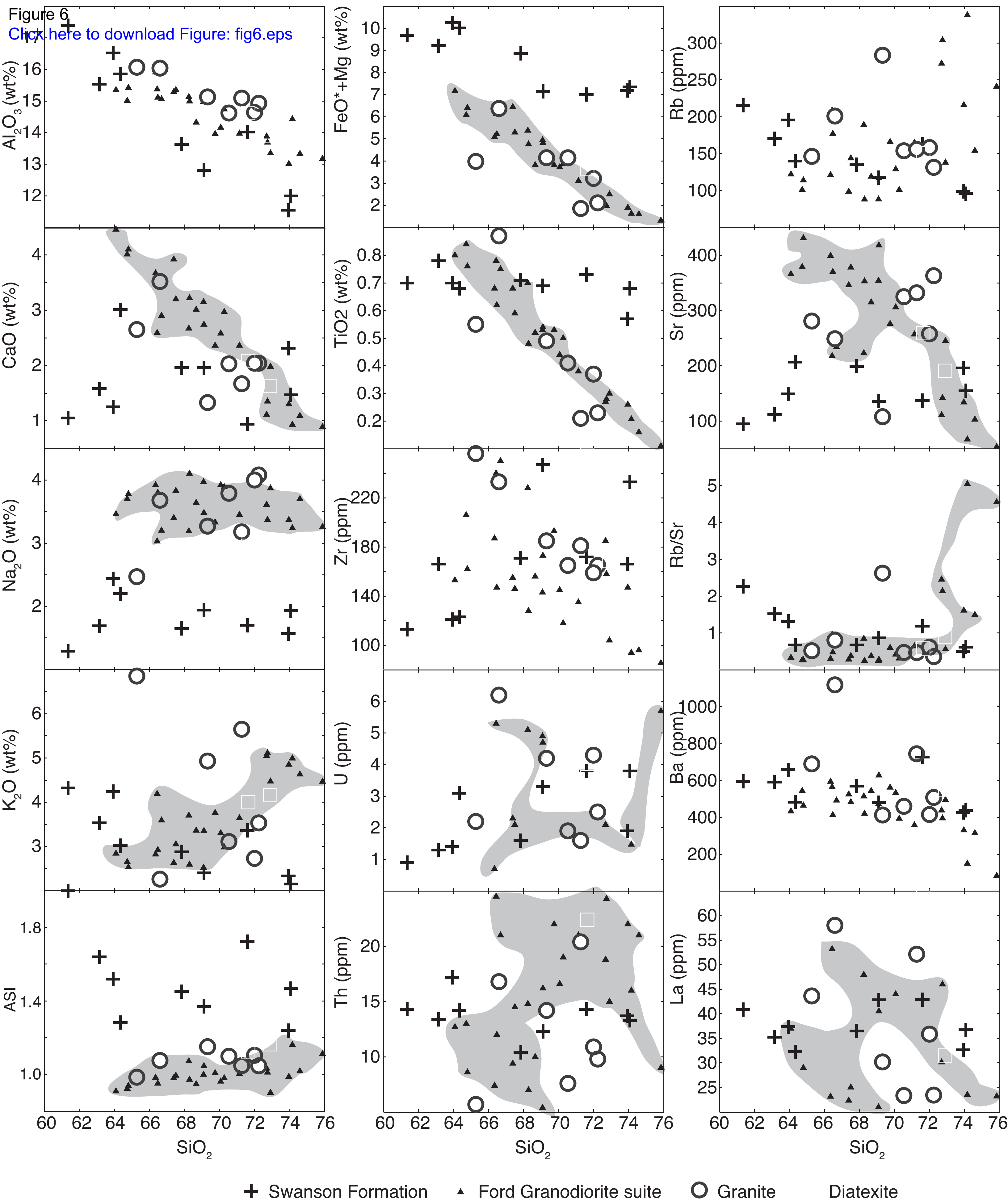


Figure 6
Yakymchuk et al.

Figure 7

Click here to download Figure: fig7_R2.eps

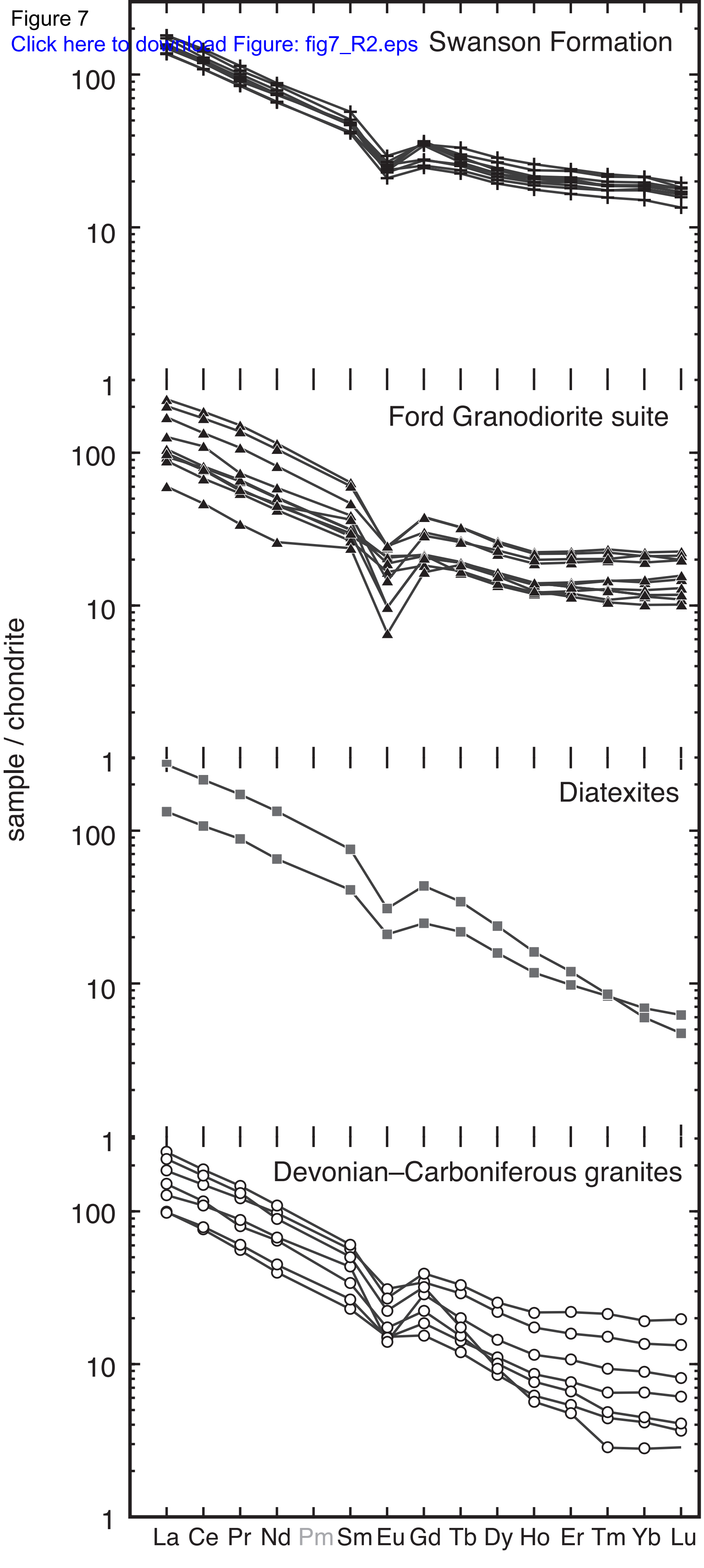


Figure 7
Yakymchuk et al.

Figure 8
Click here to download Figure: fig8.eps

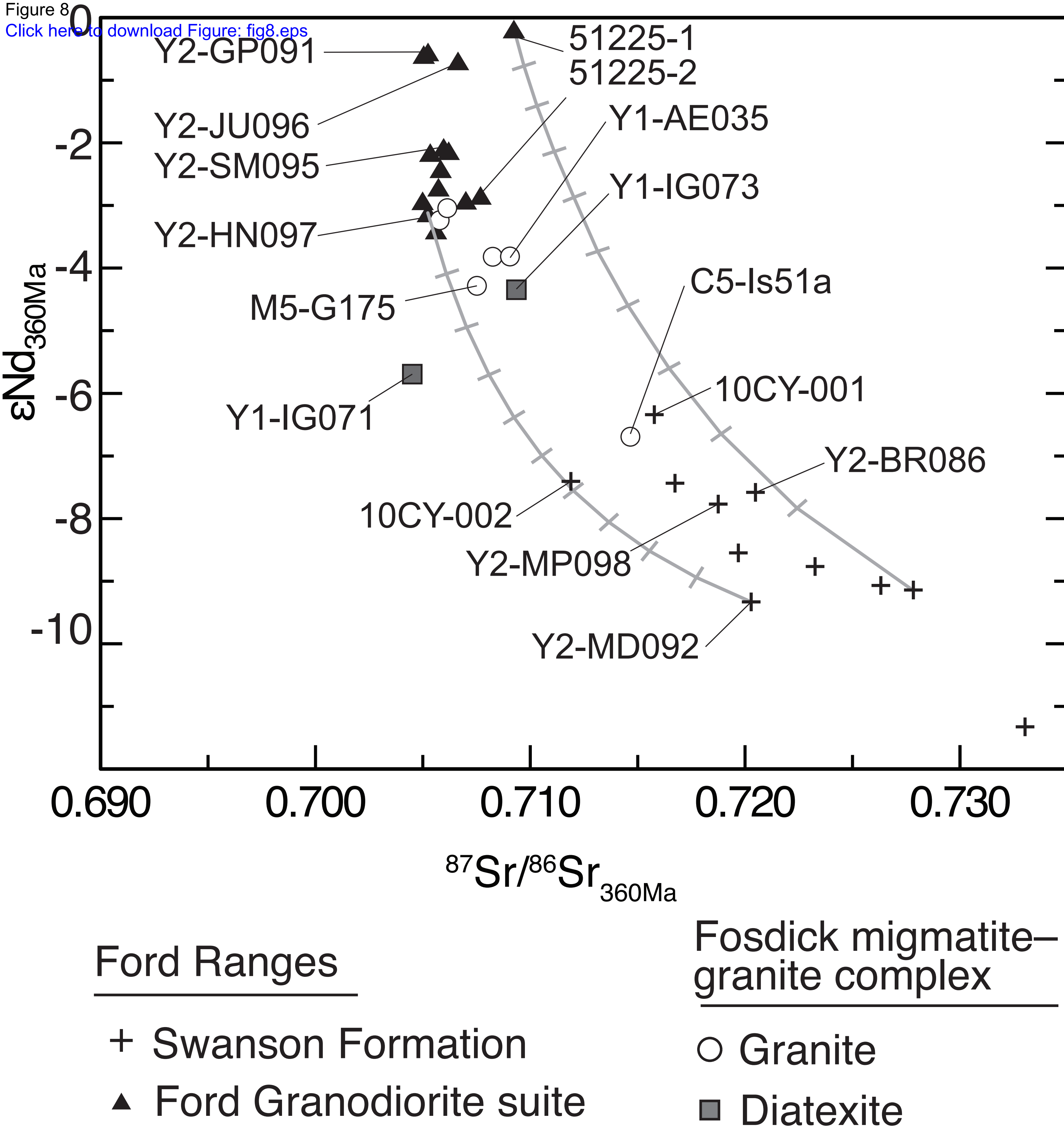


Figure 8
Yakymchuk et al.

Figure 9
Click here to download Figure: fig9_R2.eps

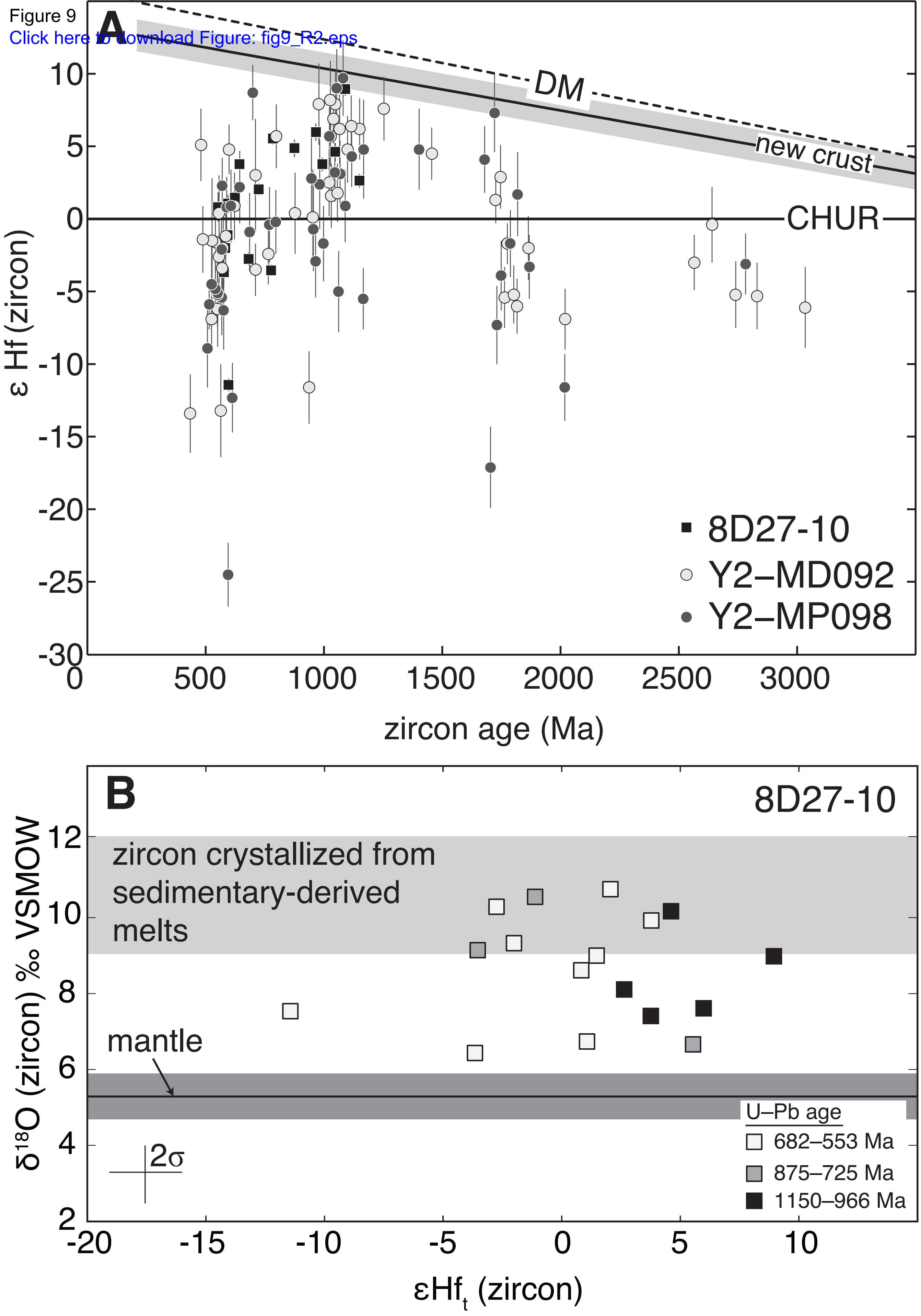


Figure 9
Yakymchuk et al.

Figure 10
Click here to download Figure: fig10.eps

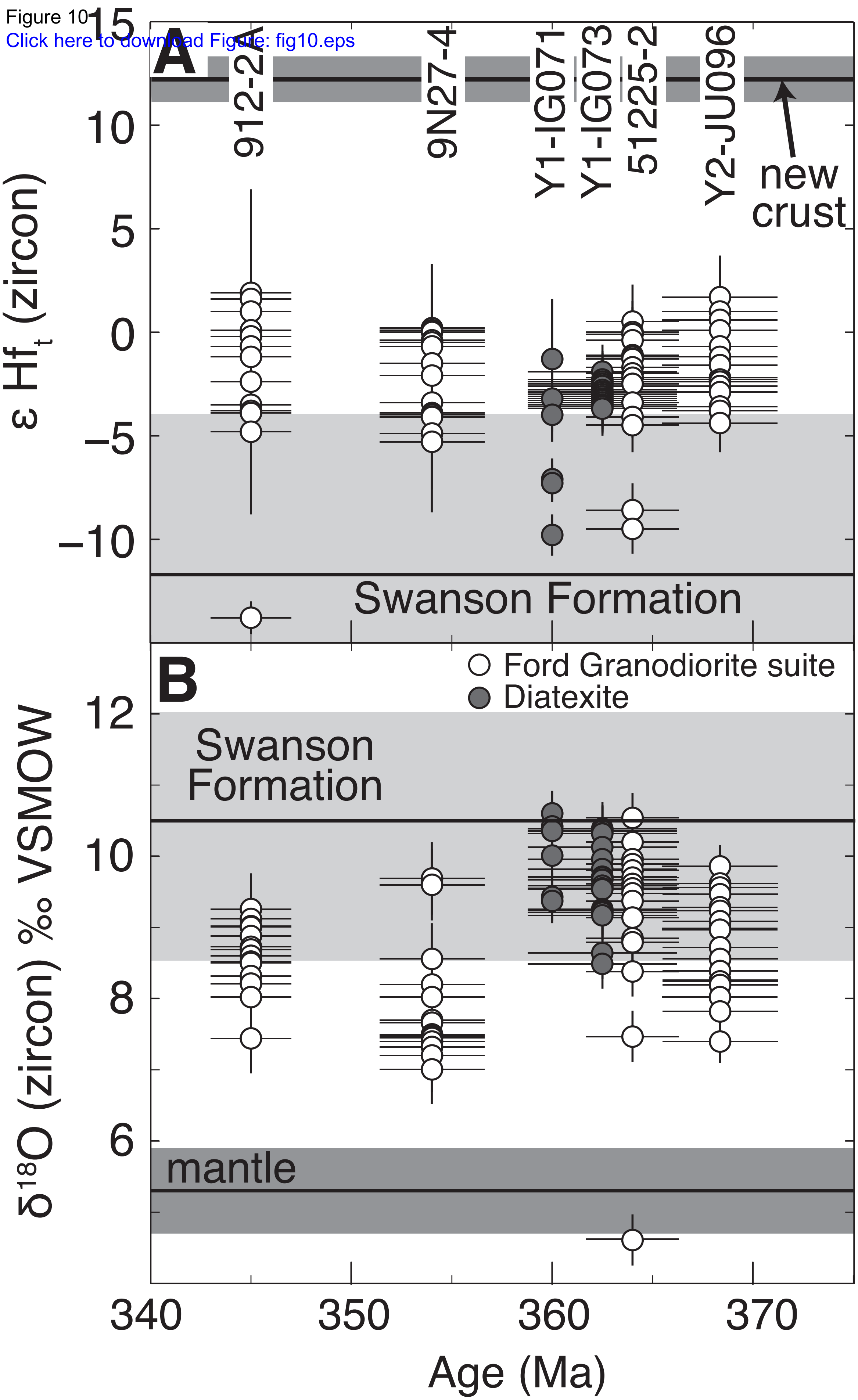


Figure 10
Yakymchuk et al.

Figure 11
Click here to download Figure: fig11.eps

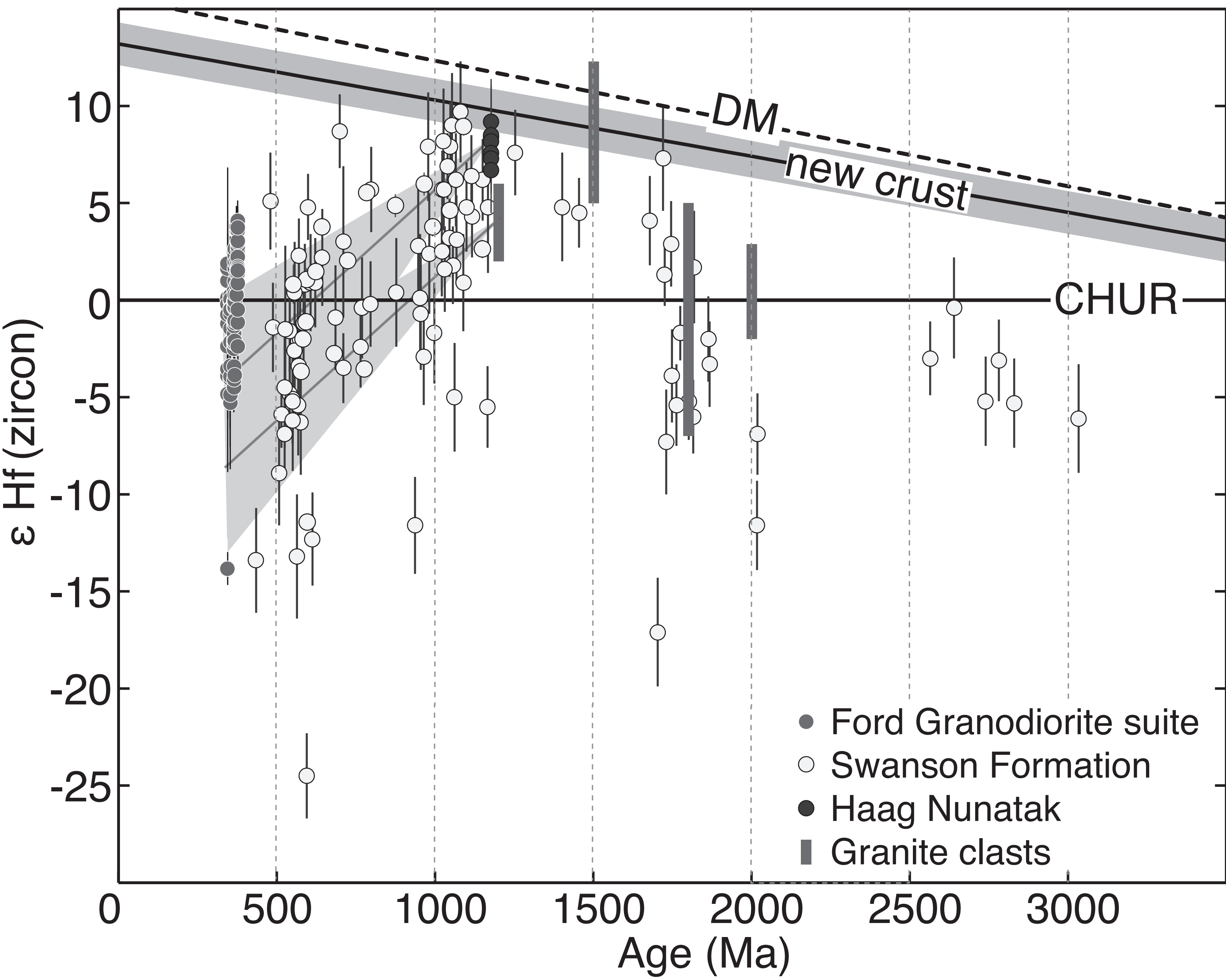


Figure 11
Yakymchuk et al.

Figure 12
Click here to download Figure: fig12.eps

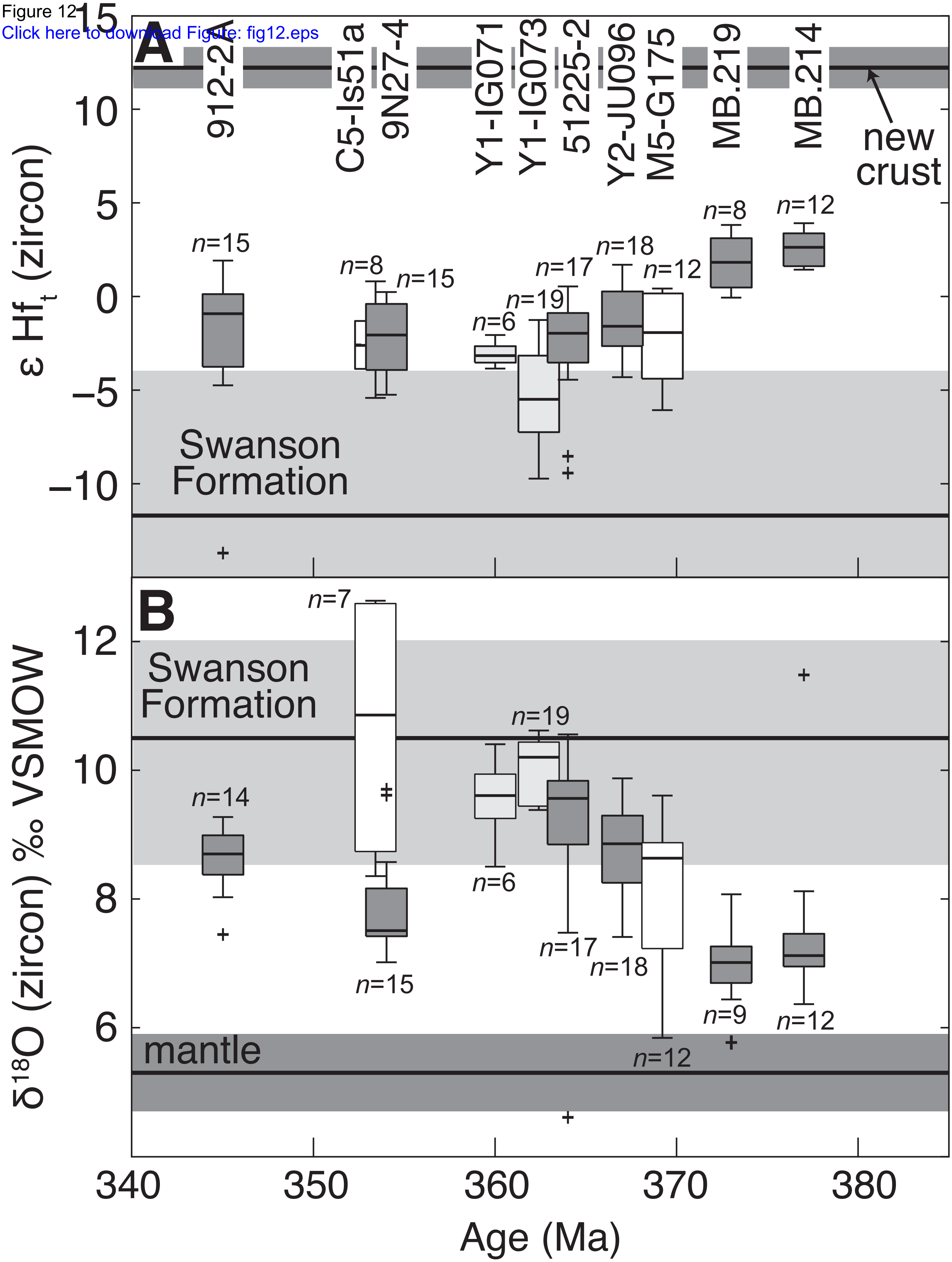


Figure 12
Yakymchuk et al.

Figure 13
Click here to download Figure: fig13.eps

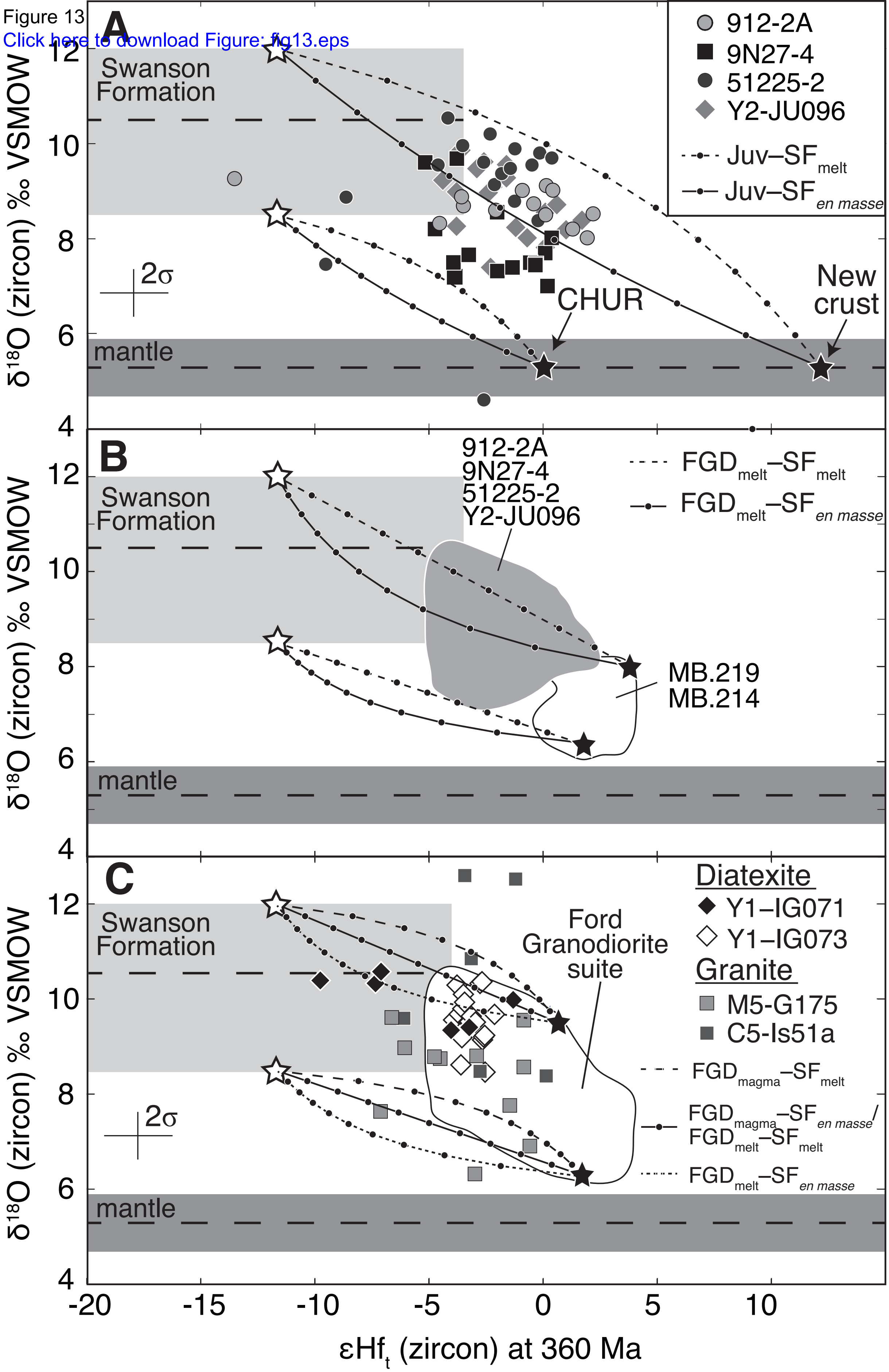


Figure 13
Yakymchuk et al.

Figure 14
Click here to download Figure: fig14.eps

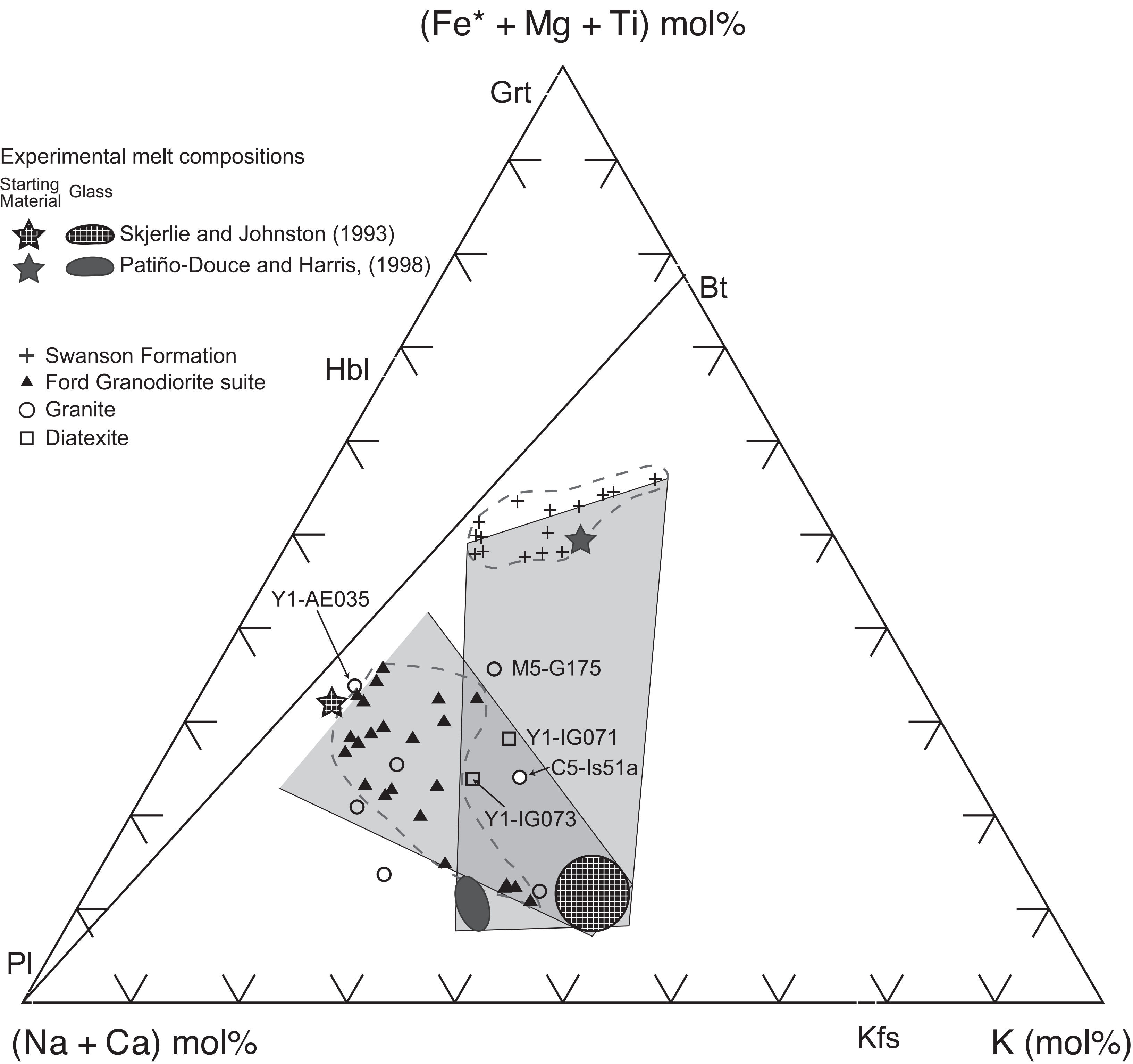


Figure 14
Yakymchuk et al.

Figure 15
Click here to download Figure: fig15.eps

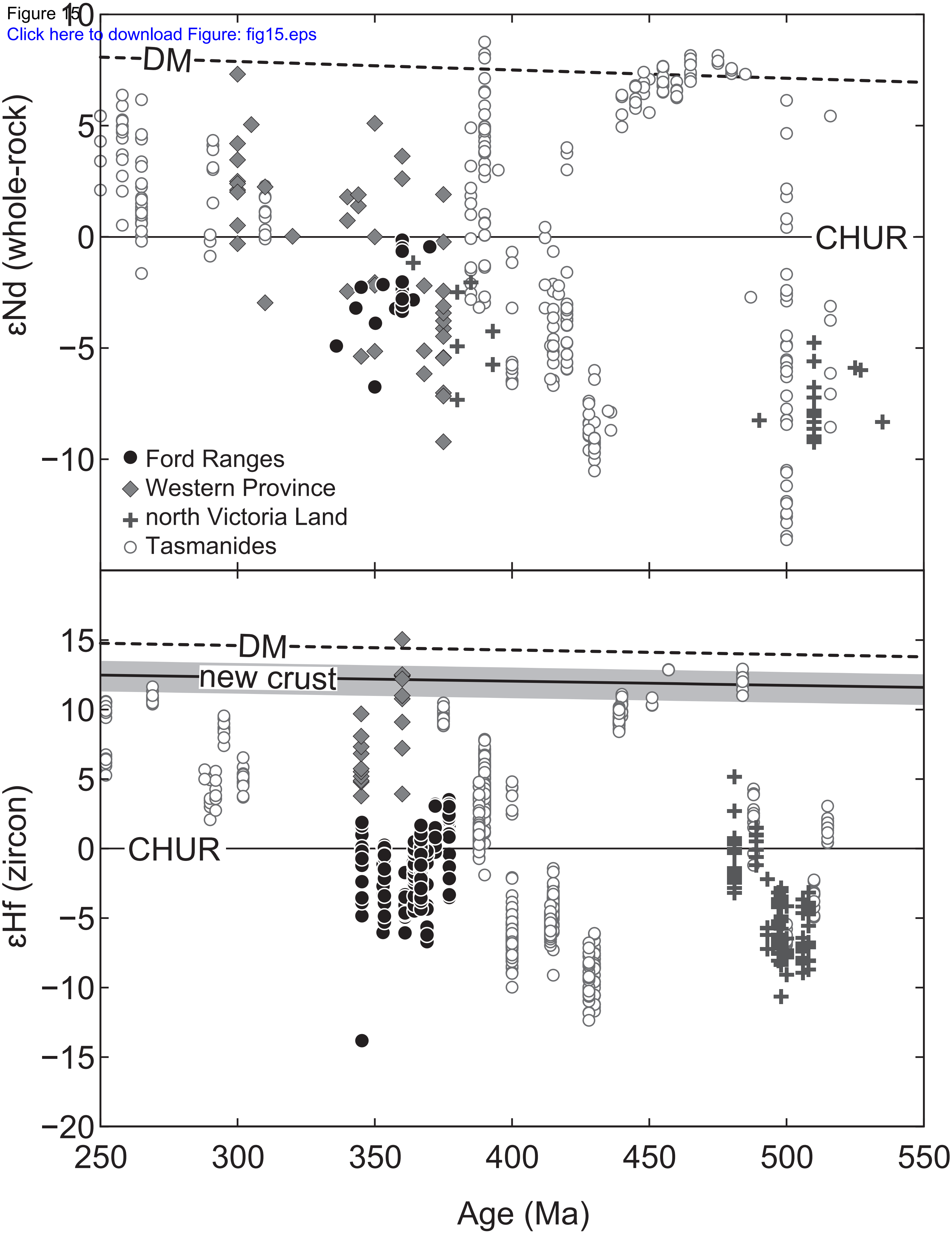


Figure 15
Yakymchuk et al.

Table 1

TABLE 1. ANALYTICAL INFORMATION BY SAMPLE

| Sample | ANU U–Pb | ANU Hf, O | U. Arizona U–Pb | U. Arizona Hf | U. Maryland Sr, Nd | U. Maryland REE |
|---|---|---|---|---|---|---|
| Swanson Formation | | | | | | |
| 10CY-001 | | | | | x | x |
| 10CY-002 | | | | | x | x |
| Y2-BR086 | | | | | x | x |
| Y2-MD092 | | | x | x | x | x |
| Y2-MP098 | | | x | x | x | x |
| 318-M9 | | | x | | | |
| 21223-3 | | | x | | | |
| 21223-8 | | | x | | | |
| 8D27-10 | x* | x* | x | | | |
| Ford Granodiorite suite | | | | | | |
| MB.214 | x† | x* | | | | |
| MB.219 | x† | x* | | | | |
| 912-2A | x | x | | | x | x |
| 9N27-4 | x | x | | | x | x |
| 51225-1 | | | x | | x | x |
| 51225-2 | x | x | x | | x | x |
| Y2-GP091 | | | x | | x | x |
| Y2-HN097 | | | | | | x |
| Y2-JU096 | x | x | x | | x | x |
| Y2-SM095 | | | | | x | x |
| Devonian–Carboniferous granite | | | | | | |
| Y1-AE035 | | | x | | x | x |
| C5-Is51a | x* | x* | | | x§ | x§ |
| M5-G175 | x* | x* | | | x | x |
| Diatexite | | | | | | |
| Y1-IG071 | x | x | x | | x | x |
| Y1-IG073 | x | x | x | | x | x |

*Yakymchuk et al. (2013a).
†Pankhurst et al. (1998).
§Korhonen et al. (2010a).

Table 2

TABLE 2. SUMMARY OF U–Pb AGES

| Sample | Technique | Rock type | Latitude | Longitude | U–Pb age (Ma) | MSWD | n | Inherited (Ma) |
|---|---|---|---|---|---|---|---|---|
| Y2-GP091 | LA–ICP–MS | Ford Granodiorite suite | 76°47'S | 144°26'W | 370.7 ± 2.8 | 1.3 | 24 of 25 | |
| 51225-1 | LA–ICP–MS | Ford Granodiorite suite | 76°40'S | 14 ° W | 370.4 ± 3.9 | 2.4 | 20 of 24 | |
| Y2-JU096 | SHRIMP | Ford Granodiorite suite | 76°15'S | 14 °16'W | 368.3 ± 2.5 | 1.5 | 19 of 22 | |
| 51225-2 | SHRIMP | Ford Granodiorite suite | 76°40'S | 14 ° W | 364.4 ± 2.3 | 1.2 | 21 of 24 | 928, 547 |
| 9N27-4 | SHRIMP | Ford Granodiorite suite | 76° 8'S | 144° 2'W | 353.5 ± 2.7 | 1.8 | 19 of 20 | |
| 912-2A | SHRIMP | Ford Granodiorite suite | 77°10'S | 144°48'W | 345.3 ± 2.0 | 0.51 | 21 of 24 | 523, 498 |
| Y1-IG071 | SHRIMP | Diatexite | 76°30'S | 145°49'W | 376–305 and 109–104 | – | – | 2277–542 |
| Y1-IG073 | LA–ICP–MS | Diatexite | 76°30'S | 145°49'W | 362.4 ± 3.7 | 2.1 | 21 of 24 | |
| Y1-AE035 | LA–ICP–MS | Granite | 76°26'S | 145°21'W | 372.3 ± 6.0 | 2.5 | 23 of 24 | |